7-2019

Bioproduction of Adipic Acid Using Engineered *Pseudomonas Putida* Kt2440 from Lignin-Derived Aromatics

Howard Willett

BIOPRODUCTION OF ADIPIC ACID USING ENGINEERED *PSEUDOMONAS PUTIDA* KT2440 FROM LIGNIN-DERIVED AROMATICS

By

Howard Willett

A THESIS

Presented to the faculty of

The Graduate College at the University of Nebraska

In Partial Fulfillment of Requirements

For the Degree of Master of Science

Major: Chemical Engineering

Under the Supervision of Professor Wei Niu

Lincoln, Nebraska

July 2019

BIOPRODUCTION OF ADIPIC ACID USING ENGINEERED *PSEUDOMONAS PUTIDA* KT2440 FROM LIGNIN-DERIVED AROMATICS

Howard Willett, M.S.

University of Nebraska, 2019

Advisor: Wei Niu

Current industrial synthesis of adipic acid is nonrenewable and depends on a carcinogenic starting material, benzene. Biocatalysis with an engineered microorganism could turn a renewable feedstock into a value-added chemical such as adipic acid. Here we engineered *P. putida* KT2440 to transform lignin-derived aromatics, coumarate and ferulate, into adipic acid. Lignin is a recalcitrant plant biopolymer burned for thermal energy. Conversion of lignin into a value-added chemical will improve the efficiency of lignocellulose processing plants. The best performing engineered KT2440 strain produces 2.52 mM adipate at a 9.5% (mole/mole) yield. This was achieved by the genetic insertion of non-natural biosynthetic pathway comprised of three enzymes and the deletion of endogenous β-ketothiolase enzymes.

Table of Contents

List of Multimedia Objects

CHAPTER 1

CHAPTER 2

CHAPTER 3

CHAPTER 1 – Background

1.1 Lignin valorization for efficient biorefineries

Today's society is reliant on petroleum for energy and, more exclusively, for a vast majority of commodity chemicals that are used to make consumer goods. Thousands of products used daily, from baby oil to practically anything plastic, are directly sourced from petroleum. The so-called petrochemicals include alcohols, aromatics, and hydrocarbon compounds.[1] Petroleum reserves are finite and cannot supply demand indefinitely. Petroleum takes millions of years to form, but is extracted and used much quicker. The consensus is certain: to continue our current way of life is unsustainable and fossil fuel-derived chemicals must be synthesized from a renewable resource or risk running out of supply.

Lignin is an untapped resource for the production of commodity chemicals. Lignin is a heterogeneous biopolymer found in the cell wall of plants. It is made by the polymerization of aromatic coniferyl alcohol (G-units), *p*-coumaryl alcohol (H-units) and syringyl alcohol (S-units) (Fig. 1-1). These units, or monolignols, are synthesized from cinnamate, which is derived from phenylalanine by the catalysis of L-phenylalanine ammonia-lyase. Cinnamate is hydroxylated at the 4' carbon position by cinnamate 4-hydroxylase to form *p*-coumaryl alcohol (H-unit). *p*-Coumaryl alcohol is converted to coniferyl and syringyl alcohol by hydroxlase and methyl transferase enzymes that attach hydroxyl and methyl groups at the 3' and 5' positions of the aromatic ring. Monolignols are transported outside the cell membrane and polymerized by a radical reaction in the cell wall.[2] The most common linkage of lignin is a β-O-4 linkage, but other carbon-carbon and carbon-oxygen bonds are also formed. This biopolymer has a molecular

weight distribution from 6,000 to 15,000 g/mole or more, depending upon the plant source. Lignin constitutes approximately 1/3 of lignocellulose by dry weight, 15-40% of plant dry weight, and 30% of organic carbon in the biosphere.[3]

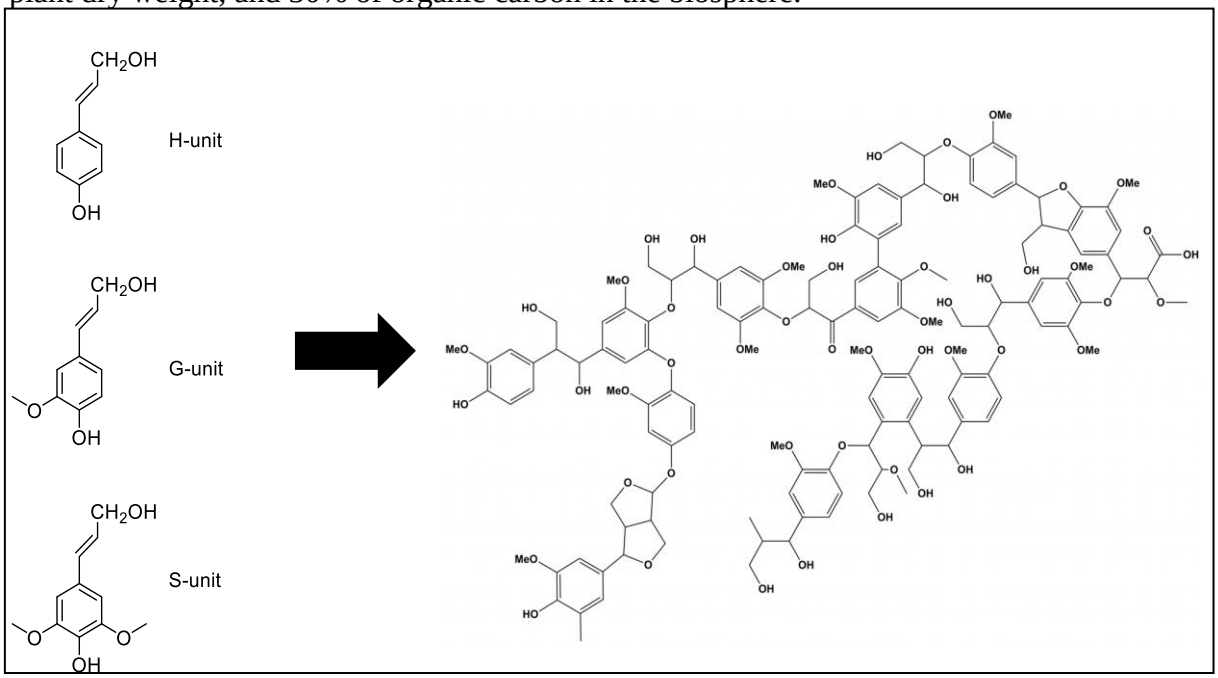

Figure 1-1. Monolignols and example lignin structure. Depicted are the three monolignols, including *p*-coumaryl alcohol (H-unit), coniferyl alcohol (G-unit), and syringyl alcohol (S-unit). These monomers are condensed into an amorphous polymer with a structure similar to the example provided. Lignin lacks a defined 3-D structure, but is a seemingly random assortment of monolignols.

Lignin is separated from cellulose and burned as a fuel due to its heterogeneity. The separation and depolymerization of lignin is its own research field. Many different methods have been developed for the treatment of lignin, such as using acid, base, ionic liquids, or hot water.[4] There is currently a surplus of lignin, as approximately 60% more is produced than needed to provide energy to lignocellulose processing plants by combustion.[2] Meeting current energy goals for U.S. biorefineries will increase the amount of biomass processed and lead to more lignin production. The surplus of lignin produced will need a purpose in order to make second-generation biorefineries more efficient. A conversion process may turn lignin-derived aromatics into a value-added

product. Current roadblocks to efficient utilization of lignin include the inherent heterogeneity of lignin and difficulties with depolymerization. Depolymerization leads to a mixture of different compounds that is difficult to characterize. Common components of lignin depolymerization products are monolignols, their conjugate acids, their conjugate aldehydes, aliphatics such as methane or ethane, and dimers, trimers and other forms of semi-polymerized lignin.[4] The exact composition is dependent on the depolymerization method used and the type of plant source.[4]

1.2 Bioproduction of small molecules

Biological systems have the ability to transform a wide variety of chemicals including sugars, waste-feedstocks, and oils to value-added chemicals. Enzymes have been purified and used as catalysts to make biological molecules and are playing important roles in today's chemical industry, in particular for the production of fine chemicals. For example, transaminase enzymes are used in many different syntheses, including the preparation of sitagliptin, which is used in the treatment of type 2 diabetes.[10,11] Due to the promising future of enzyme catalysis, the recent Nobel Prize in chemistry was awarded for the directed evolution of enzymes to improve or gain new functions.

In addition to directly using enzymes as catalysts, cell based biocatalysis has certain benefits. Cells are able to divide naturally, produce enzymes and regulate enzyme function, and avoid the costly step of enzyme purification. Cell-based biosynthetic platforms may be more stable, as the enzymes exist in an intracellular environment, which may prevent degradation of expressed proteins. Many enzymes are sensitive to oxygen. Purification may lead to oxidation, which can cause enzyme inactivation. Cells also self-propagate when given the correct nutrients, and are cultured under appropriate

conditions. Cells can express multiple enzymes, which catalyze multiple steps in a synthetic pathway. Using cells to produce a chemical is referred to as a fermentation process. Early examples of fermentation produced natural molecules. Instances of fermentation have been documented as early as 6500 B.C. in China, where ethanol was produced via fermentation for human consumption.[12] Traditionally, natural producers are stressed to induce mutations and screened for better producing phenotypes. With advances in fundamental understanding of microbial physiology and in genetic engineering methodology, almost any metabolic intermediate can be overproduced when the right genetic modifications are engineered. A natural tricarboxylic acid cycle (TCA) intermediate, succinate, has been produced by engineered *E. coli* and other strains including *Anaerobiospirillum succiniciproducens* and *Actinobacillus succinogenes*.[13] This is one academic example of hundreds of natural products that are produced by microbial fermentations.

As genetic engineering techniques have improved, the ability to engineer multiple proteins inside an organism to create new biochemical synthetic pathways has been explored. This allows non-natural products to be synthesized using engineered microbial hosts. Another petroleum-derived chemical, 1,4-butanediol (BDO), has been synthesized in this way illustrating the utility of bacterial fermentations. BDO is used industrially as a solvent, in plastics, and as a chemical intermediate to produce other chemicals. A heterologous pathway consisting of five recombinant enzymes and two endogenous enzymes was constructed in an *E. coli* strain, which is capable of producing 18 g/L BDO from renewable carbohydrate feedstock (Fig. 1-2).[14] Critical to the success of this pathway was the screening of suitable heterologous enzymes, codon optimization of

heterologous genes, and balancing of gene expression by splitting the expression of enzymes into two plasmids with different copy numbers. Deletion of chromosomal genes minimized flux into competing pathways for the biosynthesis of lactate, formate, and ethanol, as well as allowed the TCA cycle to function under micro-aerobic and anaerobic conditions.[14]

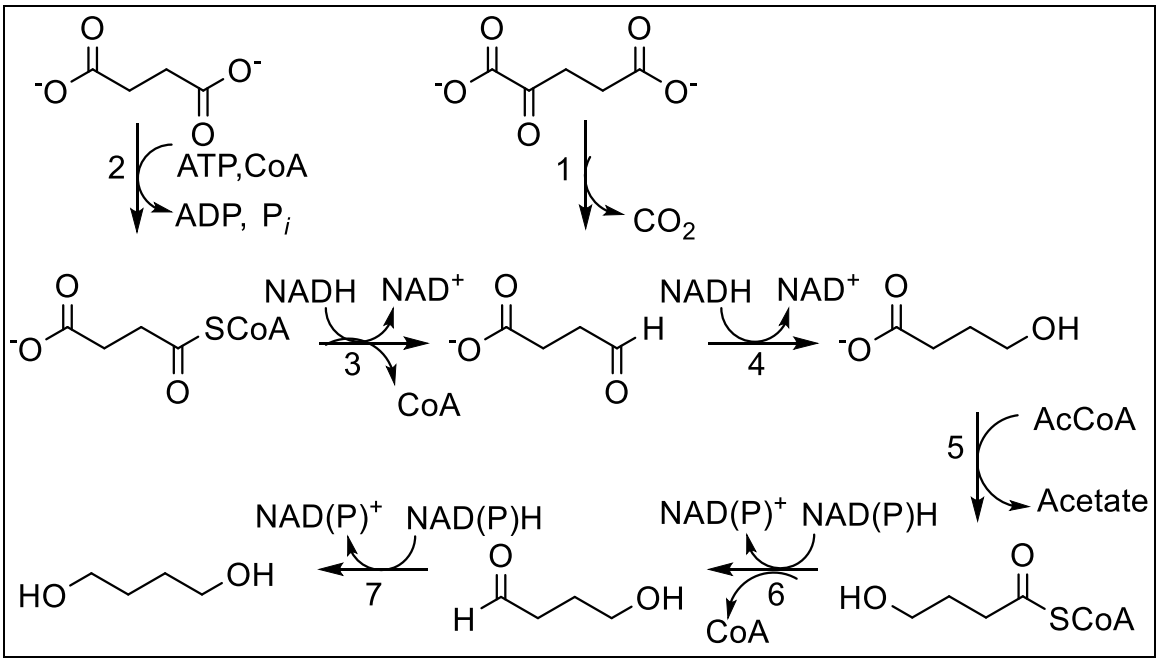

Figure 1-2. Synthetic pathway for the microbial production of 1,4-butanediol. Enzymes are 1, 2-oxoglutarate decarboxylase; 2, succinyl-CoA synthetase; 3, CoA-dependent succinate semialdehyde dehydrogenase; 4, 4-hydroxybutyrate dehydrogenase; 5, 4-hydroxybutyryl-CoA transferase; 6, 4-hydroxybutyryl-CoA reductase; 7, alcohol dehydrogenase. Enzymes 2 and 7 are endogenous to *E. coli*. Succinate and α-ketogluturate are produced naturally in the TCA.

Hosts other than *E. coli* are of interest to engineers as well and can be chosen for a variety of parameters, including unique metabolisms, solvent tolerances, or the easiness of genetic manipulations. *Saccharomyces cerevisiae*, the model single-cell yeast strain, has been engineered for the *de novo* production of resveratrol, an antioxidant compound in grapes, from glucose by introducing a biosynthetic pathway consisting of tyrosine-ammonia lyase, 4-coumaryl-CoA ligase, and resveratrol synthase, which are naturally

expressed in one microbe and two different plant species, respectively[15] The production of small molecules using engineered microbial host strains is a growing field with seemingly infinite possibilities.

1.3 *Pseudomonas putida* KT2440 and its aromatic degradation capabilities

A microbial host with a lot of academic and industrial interest is *P. putida* KT2440. *P. putida* KT2440 is a gram-negative microorganism derived from the type strain of *P. putida* by curing of the TOL plasmid, a plasmid for toluene degradation. KT2440 has a wide-range metabolism and is able to degrade many compounds such as trinitrotoluene (TNT), propanediol, and taurine.[5] It is a root-associated microorganism. KT2440 degrades glucose through the Entner-Doudoroff pathway leading to higher levels of reducing cofactors. It lacks 6-phosphofructokinase forcing it to degrade glucose through the Enter-Doudoroff pathway. KT2440 has an intact gluconeogenesis pathway up to glucose-6-phosphate.[6]

KT2440 is considered as an attractive future platform strain due to its ability to degrade lignin-derived aromatics (LDA), it is amenable to genetic manipulation, and its status as a Generally Recognized As Safe (GRAS) strain. KT2440 is able to degrade aromatic compounds and funnel them to protocatechuate or catechol via peripheral pathways. Mandelate, toluene, tryptophan, anthranilate, cinnamate, phenol, benzene, aniline, salicylate, and naphthalene are broken down into catechol, while other aromatic compounds like *p*-coumarate, *p*-cresol, 3-hydroxybenzoate, coniferyl alcohol, vanillate, and ferulate are converted into protocatechuate acid (PCA).[7] This funneling feature may allow KT2440 to turn a feedstock comprised of multiple phenolic compounds, such as depolymerized lignin, into one value-added commodity chemical.

The β-ketoadipate pathway converts both PCA and catechol into β-ketoadipate (Fig. 1-3).[7] β-ketoadipate is then broken down into succinyl-CoA and acetyl-CoA. These molecules are degraded through central metabolism. The β-ketoadipate pathway, as well as the peripheral pathways to degrade ferulate, coumarate, and vanillate, is present in *P. putida* KT2440.[8] These aromatic compounds are of particular interest because of their structural similarity to monomers in lignin and presence in depolymerized-lignin feedstocks. *P. putida* KT2440 could take depolymerized lignin and convert the G and H unit derived species into β-ketoadipate (BKA). Sinapic acid is theoretically demethylated into gallic acid. which is broken down via a separate Gal gene cluster that does not generate β-ketoadipate as an intermediate, but there are no published reports of sinapic acid utilization in *P. putida*.[9]

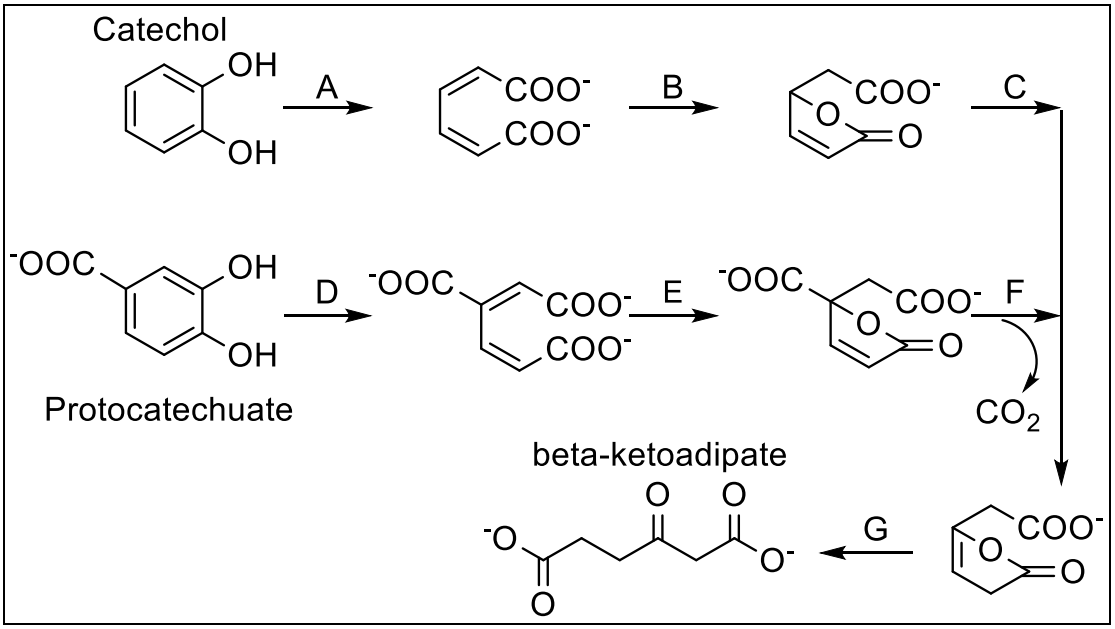

Figure 1-3. β-ketoadipate pathway in prokaryotes. Aromatics rings in catechol and protocatechuate are opened in oxygen-dependent reactions catalyzed by A. catechol-1,2-dioxygenase and D. protocatechuate-3,4-dioxgenase. Further reactions are catalyzed by B. *cis,cis*-muconate lactonizing enzyme; E. β-carboxy-*cis,cis*-lactonizing enzyme; C. β-carboxymuconolactone isomerase ;F. muconolactone isomerase; G. β-ketoadipate enol-lactone hydrolase;

1.4 Current industrial production of adipic acid

Adipic acid is a six carbon dicarboxylic acid. It has a market volume of approximately 3 million tons per year with a projected growth of 3% annually.[16] Adipic acid is the most important industrial dicarboxylic acid, owing to its use in the synthesis of Nylon-6,6, which is a polyamide fiber formed after the condensation between adipic acid and hexamethylenediamine. Nylon-6,6 is used in many products, ranging from textiles, carpets, to electric-insulating materials, hoses, conveyor belts, and more. Nylon-6,6 represents 61% of global adipic acid consumption. Nylons (nylon-6,6 and other derivatives) account for approximately 1% of global polymers with an expected $30 billion market in 2020.[17] Other than nylon, adipic acid is also used as a plasticizer, food additive, and as a building block to synthesize other chemicals and polymers.

Current production of adipic acid relies on petroleum-derived benzene as a starting material. Benzene is a known carcinogen, making it an undesirable starting material.[18] In a process developed by DuPont, benzene is hydrogenated into cyclohexane, which is oxidized into a cyclohexanol/cyclohexanone mixture called KA oil. This KA oil is then further oxidized with nitric acid to form adipic acid. This synthetic route accounts for 93% of the global adipic acid produced. In addition to relying on nonrenewable starting material, adipic acid synthesis produces nitrous oxide, a greenhouse gas, as a byproduct. More recently, catalytic scrubbers, reduction or recovery technologies have been included to reduce the environmental impact of adipic acid production by mitigating nitrous oxide release.[19] Other synthetic routes have been investigated and developed but have not been implemented at the industrial scale as the DuPont process (Fig. 1-4).

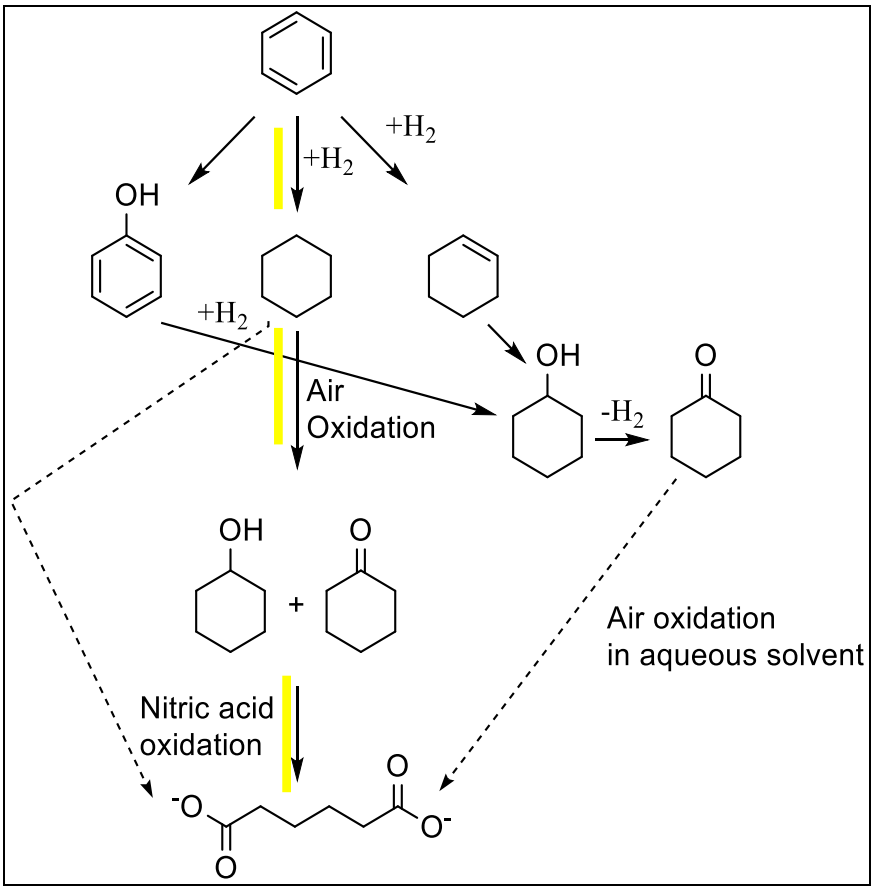

Figure 1-4. Adipic acid chemical synthetic routes. Chemical synthesis for adipic acidthat are in industrial use (solid line). Chemical synthesis that are shown as proof-ofconcept schemes (dashed line). DuPont process that accounts for 93% of adipic acid produced is highlighted in yellow. Figure is adapted from ref 16.

These syntheses are grouped into four major types: phenol (cyclohexanol), cyclohexane, cyclohexene, and butadiene carbonylation routes (not shown).[16] More exotic synthetic pathways routing through adiponitrile or tetrahydrofuran have also been developed, but they have not gained industrial traction due to the lack of cost competitiveness to the traditional synthesis.[16]

1.5 Bio-adipic acid

The prospect of bio-adipic acid was illustrated almost 20 years ago. Niu *et al*. engineered a strain of *E. coli* to produce 36.8 g/L *cis,cis*-muconic acid from glucose in 48 h.[20] Muconic acid be chemically reduced into adipic acid. In this pathway, native

biosynthesis of aromatic amino acids was hijacked to convert 3-dehydroshikimic acid, a biosynthetic intermediate, into PCA. PCA is decarboxylated into catechol, which is oxidized into *cis,cis*-muconic acid.[20] The last three enzymatic steps are catalyzed by heterologous enzymes expressed in an *E. coli* strain engineered for increased flux through the aromatic amino acid biosynthesis pathways. This strategy of muconic acid production was mimicked in *S. cerevisiae*, which achieved a titer of 141 mg/L.[21]

Alternatively, the direct biosynthesis of adipic acid from carbohydrates has been demonstrated via reverse adipate degradation pathway. In this pathway, succinyl-CoA and acetyl-CoA are condensed into β-ketoadipoyl-CoA. The β-ketoadipoyl-CoA is converted to adipoyl-CoA via reverse beta-oxidation reactions and then further converted to adipate.[22] Recently this pathway has been introduced into *E. coli* and reached a yield of 93.1% of the maximum yield. In order to achieve this, genetic deletions to remove competing pathways and to increase the concentration of succinyl-CoA were engineered.[23] Another pathway for bio-adipic acid has been patented by Genomatica that routes through α-ketoadipate which is converted to adipate in similar reactions to β-ketoadipoyl-CoA. Advanced pilot or demo sized plants have been developed by Rennovia, Inc and Verdezyne, Inc. [22] Rennovia's bio-adipic acid is made by chemical reduction of glucaric acid, which is produced chemo-catalytically from bio-based started materials. Verderzyne is no longer operating as a company, but their biosynthetic pathway converts long-chain oils into adipate via ω-oxidation and chain shortening. [24]

Multiple organisms, including *Pseudomonas putida*, have been engineered to convert cyclic feedstocks, including benzoate, cyclohexanol, or toluene into *cis,cis*-muconic acid. Conversion of toluene or catechol into muconic acid was first patented in

1982 by the Calgene Corporation.[25] They describe a KT2440 strain that was deficient in muconate lactonizing enzyme, thereby over accumulating *cis,cis*-muconate via the breakdown of substrates through the catechol branch of the β-ketoadipate pathway. These pathways suffer from the same problems as chemo-catalytic conversion, including the sustainability of the feedstocks and the toxicity of starting materials.[22] Cell-based pathways to bio-adipic acid are summarized in Fig. 1-5. An engineered KT2440 strain could convert lignin-derived chemicals into β-ketoadipate and biomass. The H and G units of lignin would be converted to β-ketoadipate and then converted to adipate. KT2440 could be engineered to utilize S units to grow on. Ideally, the engineered strain could grow on a depolymerize lignin source while simultaneously converting H and G units into adipate without the need of an additional carbon source.

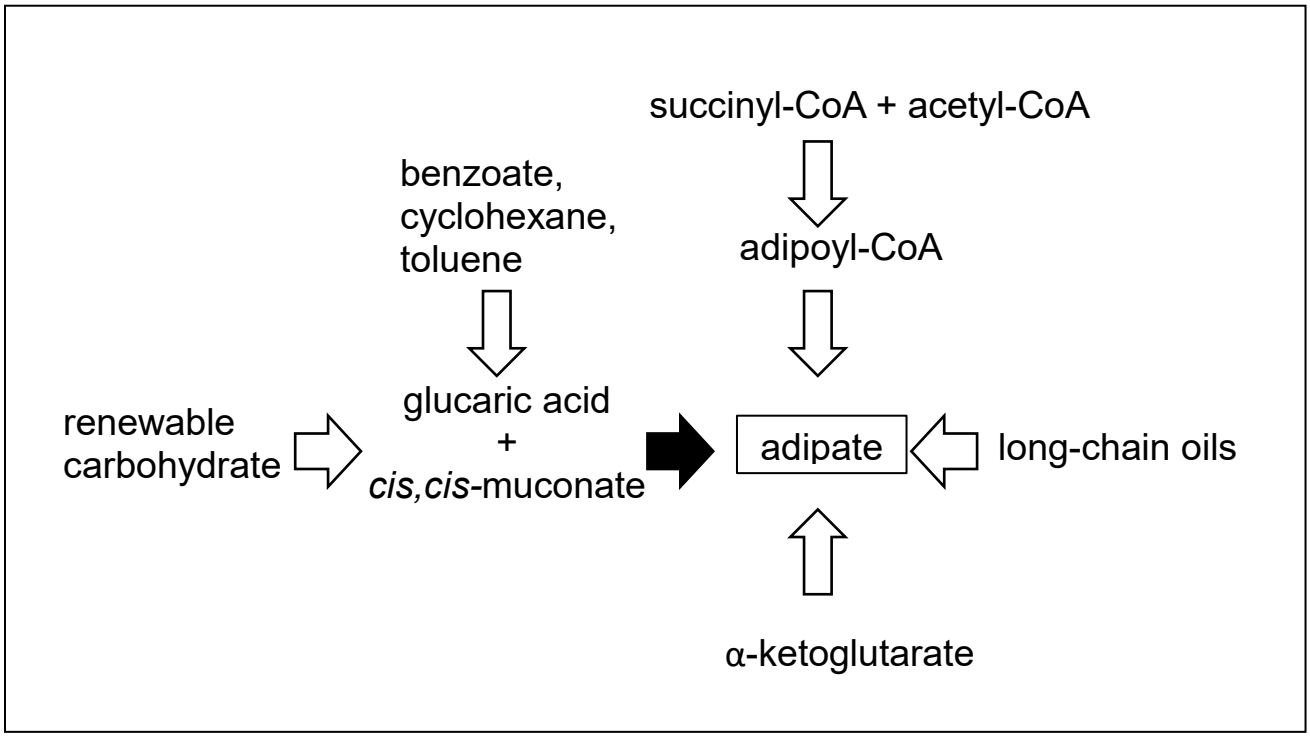

Figure 1-5. Bio-adipic acid synthesis. Black arrows indicate chemical conversion. White arrows indicate conversion by an engineered microorganism.

CHAPTER 2 - Expanding the Aromatics Metabolism Capability of *Pseudomonas putida* KT2440

2.1 Examining *P. putida* KT2440 growth on lignin-derived aromatics

It is well documented that *P. putida* KT2440 is capable of degrading G-and H-lignin-derived aromatic compounds, including ferulate and coumarate. These compounds are first activated as their corresponding CoA thioesters, then shortened by the removal of an acetyl-CoA unit. The resulting product of coumarate, 4-hydroxybenzoic acid, is hydroxylated at the meta position to give protocatechuic acid (PCA) (Fig. 2-1). The product of ferulate, vanillate, is demethylated at the meta position to convert a methoxy group into a hydroxyl group and forming PCA. PCA is oxidized by the catalysis of protocatechuate-3,4-dioxygenase and then further broken down into β-ketoadipate via the β-ketoadipate pathway (Fig 1-2).

To compare growth characteristics on different carbon sources, the wild-type KT2440 strain was examined for growth on syringate, sinapate, vanillate, coumarate, ferulate, glucose, and acetate as the sole carbon source, respectively (Fig. 2-2). Similar lag phases were observed for all carbon sources except acetate, on which the cells started growing almost immediately. The specific growth rate on each carbon source was calculated as the slope of a straight line obtained by plotting the natural log of the cell density at the exponential growth phase against time. Doubling time was calculated by using the following equation. KT2440 grew the fastest on glucose, followed by coumarate and acetate. It grew the slowest on ferulate and vanillate (Table 2-1).

$$Doubling\ Time = \frac{ln(2)}{specific\ growth\ rate}$$

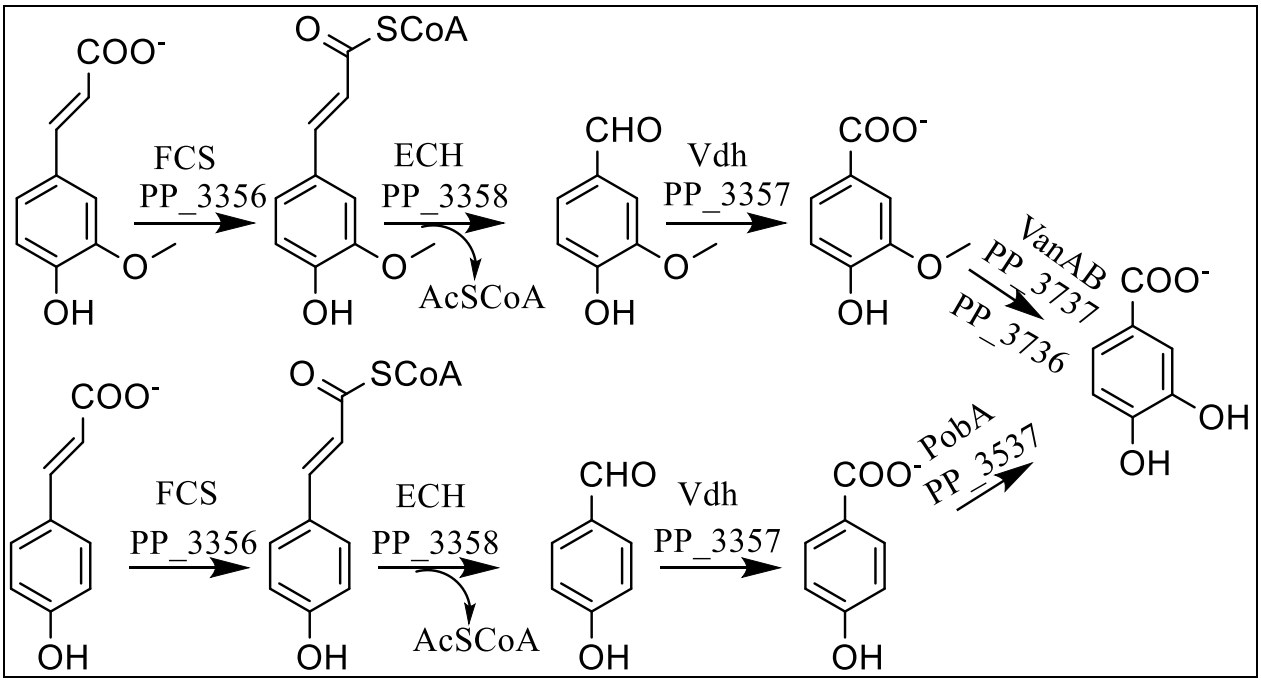

Figure 2-1. Funneling pathways for *p*-coumarate and ferulate. Pathway for ferulate degradation is shown at the top; pathway for coumarate shown on the bottom. The same genes catalyze removal of acetyl-CoA unit, the final step is catalyzed by different genes.

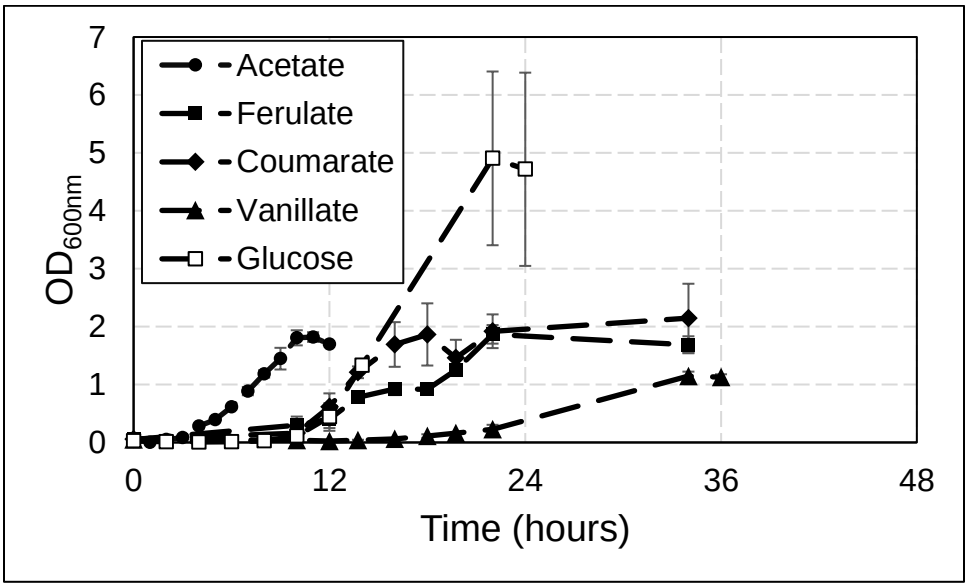

Figure 2-2. Growth curves of wild-type *P. putida* KT2440 in minimal media containing indicated carbon source. The concentration of all carbon sources was at 0.25% (w/v), except for glucose at 0.5% (w/v).

Table 2-1. Growth of wild-type *P. putida* KT2440 on various carbon sources.

	Doubling Time (minutes)	Specific Growth Rate (hr^{-1})
Coumarate	106 ± 9	0.39 ± 0.03
Ferulate	289 ± 50	0.15 ± 0.03
Vanillate	189 ± 36	0.23 ± 0.04
Glucose	63 ± 2	0.65 ± 0.02
Acetate	102 ± 8	0.39 ± 0.03

[a.] The concentration of all carbon sources was 0.25% (w/v), except for glucose, which was 0.5% (w/v)

The wild-type KT2440 strain was examined for growth on S-lignin-derived aromatic acids, including syringate and sinapate. There is no literature report on metabolism of either compound by KT2440, although the metabolism of another aromatic acid, gallate, was reported.[26] While the OD_{600nm} increased during culture experiments on syringate and sinapate, no cell accumulation was observed, as no cell pellet was obtained when cultures were centrifuged. It was noted that syringate and sinapate could be quickly oxidized to result in darkened color of culture media, which led to the increase of light absorbance. Further experiments were carried out by including 2 mM L-cysteine in the media to minimize carbon source oxidation. This was proven to be effective for approximately 48 h by monitoring OD_{600nm}.

2.2 Engineering S-lignin-derived carbon source utilization through manipulating the expression of VanAB

Metabolism of sinapate and syringate was reported in bacterial strains, such as *Sphingobium sp.* SYK-6 and *Novosphingobium aromaticivorans*. [27,28] Sinapate is activated as corresponding CoA ester and then shortened by the removal of an acetyl-CoA unit into syringate. Above steps are similar to the metabolism of coumarate and ferulate by KT2440 (Fig. 2-1). Syringate is demethylated into 3-*O*-methylgallate

(3OMG), which is further demethylated into gallate (Fig. 2-3), and then broken down by a dioxygenase enzyme that is independent of the β-ketoadipate pathway.

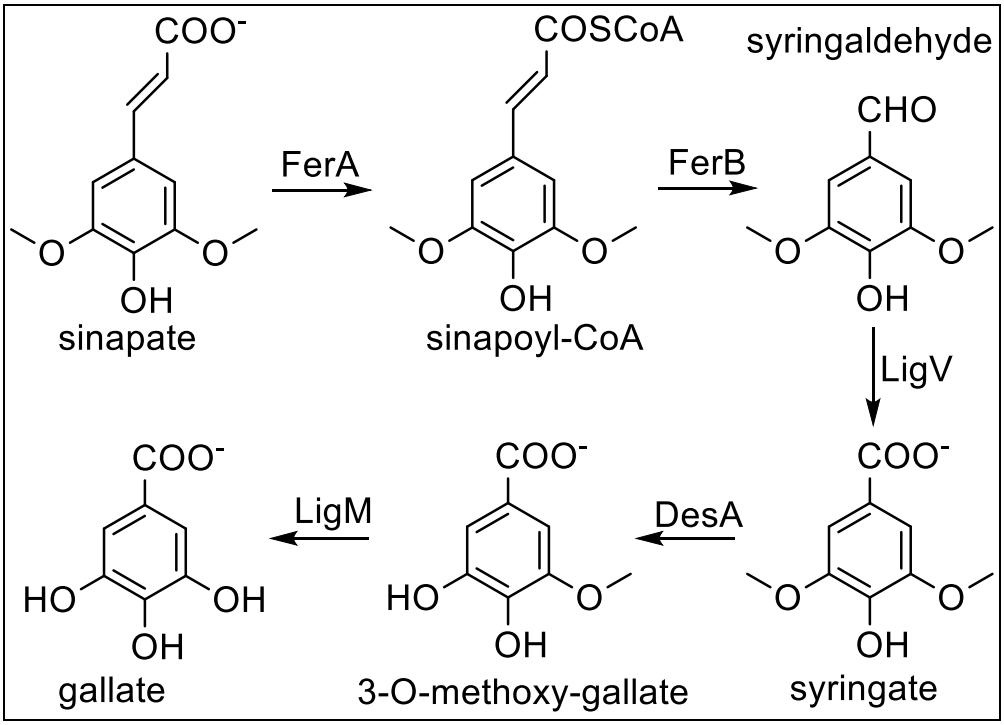

Figure 2-3. Metabolism of syringic acid. Degradation of sinapate and syringate as present in *N. aromaticivorans.*

To engineer *P. putida* for the utilization of S-lignin-derived chemical, the demethylase in KT2440 that converts vanillate into PCA, VanAB, was first investigated for possible promiscuous activity on syringate and 3OMG. *E. coli* strain BL21(DE3) was transformed with a pET28a-derived plasmid encoding VanAB. Cells were grown in M9 media. The expression of VanAB was induced at an OD_{600nm} value of 0.8. Four hours after induction, cells were pelleted and washed with M9 media, then suspended in media supplemented with 5 mM of carbon source (vanillate, 3OMG, or syringate) and 0.5% (w/v) glucose. Carbon source utilization was monitored every hour for three hours for the demethylation of vanillate, 3OMG, or syringate into PCA, gallate, or 3-OMG,

respectively. All three carbon sources were demethylated, with the highest activity on vanillate and lowest activity on 3OMG (Fig. 2-4). Experiments were first done in *E. coli* as opposed to *P. putida*, because *E. coli* lacks the necessary pathways to breakdown aromatics such as PCA, vanillate, and gallate. Since only low demethylation was observed for 3OMG, it is possible that any decrease in 3OMG may be due to oxidation. For vanillate and syringate, approximately 50% of the carbon source was demethylated in the 3 hour experiment. The experiment showed that the VanAB enzyme of KT2440 is functional for the demethylation of known intermediates in the breakdown of sinapate/syringate.

It was hypothesized that the expression of VanAB in KT2440 is regulated by repressor protein, VanR, based on homologues in other microorganisms.[29]. In the presence of ferulate, vanillin, and vanillate, the VanAB expression is induced.[30] To examine the VanAB activities on syringate and 3OMG in KT2440, the strain was grown on syringate in the presence of ferulate. However, due to signal overlap in ^{1}H NMR analysis, the, results were inconclusive. The constitutive expression of VanAB in KT2440 was then achieved by transforming the strain with a plasmid that encodes VanAB. The obtained KT2440 strain was then grown in M9 minimal media containing 12 mM syringate and 0.25% (w/v) glucose. This experiment was monitored for metabolite accumulation. Constitutive overexpression of VanAB in KT2440 allowed the complete consumption of syringate. As an intermediate of the metabolism, 3OMG was transiently accumulated (Fig. 2-5). The utilization of syringate was only observed in cells that overexpressed VanAB, which further confirmed the feasibility of engineering S-

lignin-derived aromatics utilization in KT2440 through manipulating the endogenous activity of VanAB.

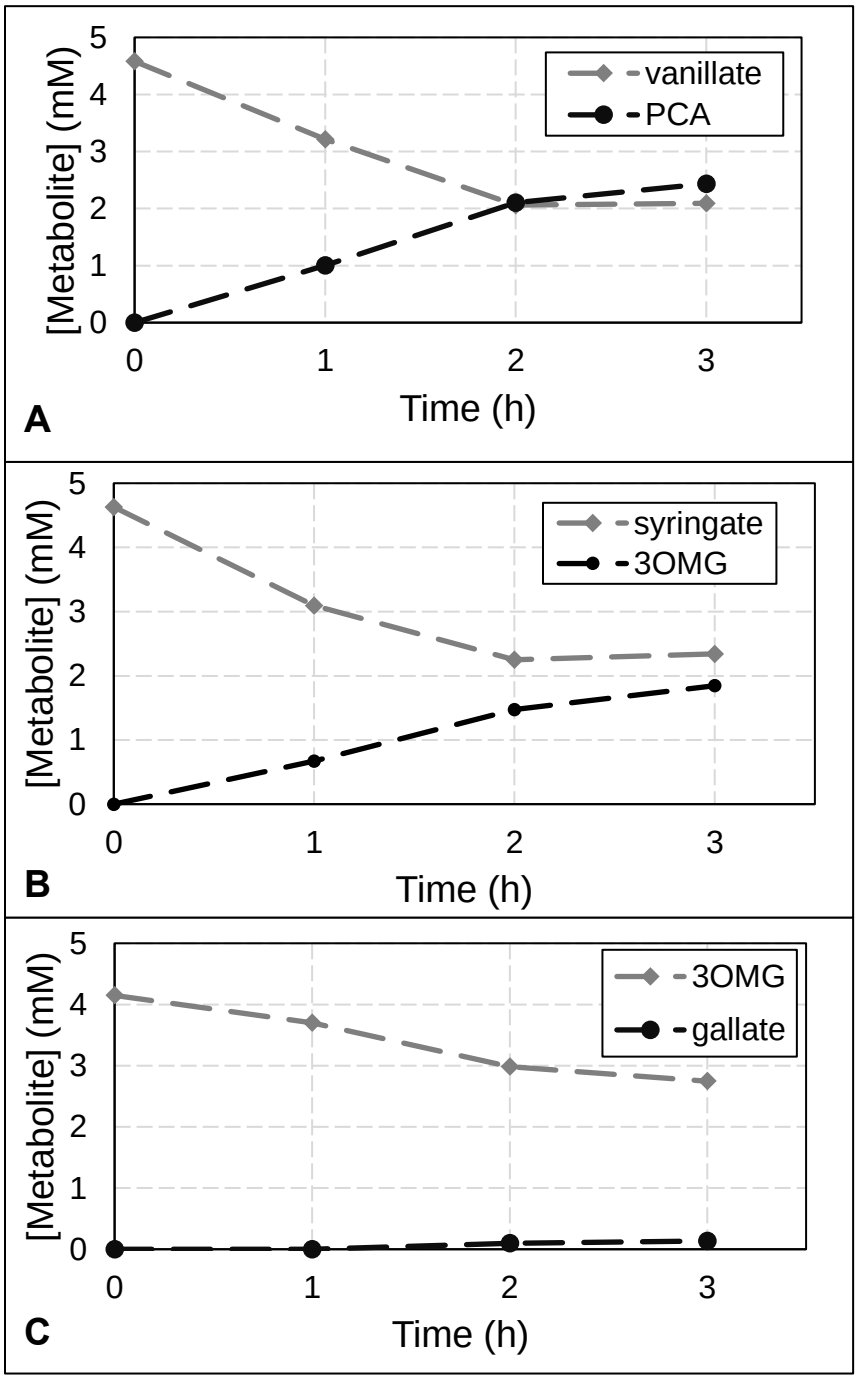

Figure 2-4. Examining the catalytic promiscuity of VanAB. Cells were grown in media containing 0.5% (w/v) glucose and 5 mM aromatic carbon source: A, vanillate; B, syringate, C, 3OMG. Metabolites monitored via ^{1}H NMR. Experiments were done in single trial. 3OMG, 3-O-methylgallate; PCA, protocatechuic acid

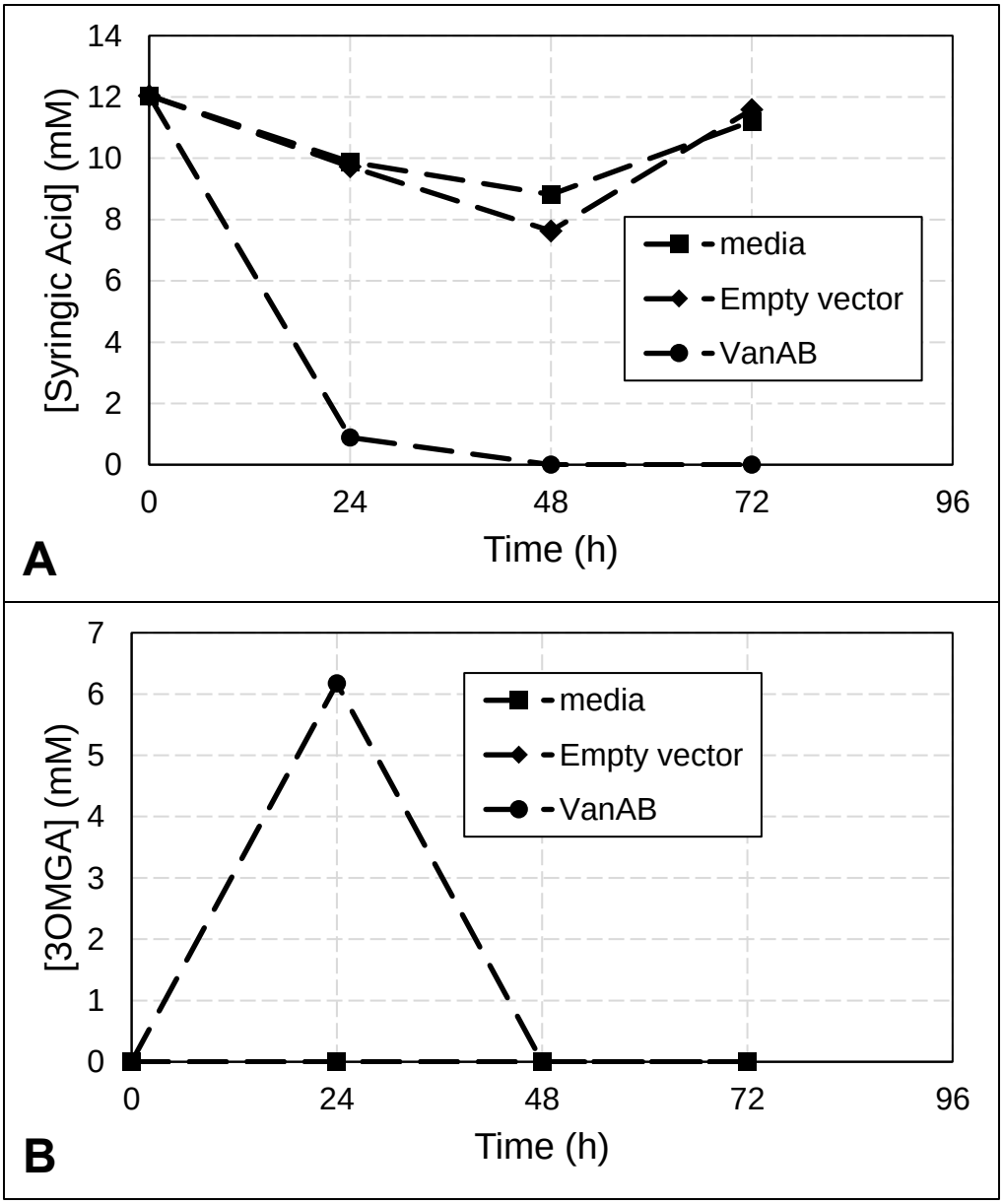

Figure 2-5. Syringate utilization with VanAB overexpression in KT2440. Cells grown in minimal media containing 0.5% (w/v) glucose and 0.25% (w/v) syringate. Metabolite accumulation monitored via ^{1}H NMR. 'Media' is a media only blank containing no cells. 'Empty vector' is a control transformed with an empty vector. A, syringate; B, 3OMG. Experiment was done in single trial.

2.3 Engineering S-lignin-derived carbon source utilization through heterologous pathway expression

An alternate approach to expand the metabolizable carbon source of KT2440 into S-lignin-derived aromatics is to heterologously express enzymes that function in the metabolism of syringate and sinapate in other bacteria, such as *Novosphingobium aromaticivorans* (Fig. 2-3).[28] The genes encoding these pathways were cloned into two separate vectors with the help of other members of our laboratory. One plasmid encodes enzymes to degrade sinapate into syringate (FerA, FerB, LigV), while the second plasmid encodes enzymes to degrade syringate into gallate (DesA, LigM). The plasmid containing *desA* and *ligM* was transformed into wild-type *P. putida* KT2440. The obtained strain was grown in minimal media containing 0.25% (w/v) syringate as the sole carbon source. No difference in the utilization of syringate was observed between the control and cells with DesA and LigM expression (Fig. 2-6) Metabolic intermediate, including 3OMG and gallate was not observed. No cell growth was observed, either. Increase in OD_{600nm} was attributed to the oxidation of starting material.

A control for this experiment was conducted in vanillate. Vanillate was chosen as a control because the cells should be able to demethylate vanillate naturally (Fig. 2-7). A growth defect was observed for the strain expressing DesA and LigM. This could be caused by the metabolic burden of expressing proteins or maintaining the plasmid. Proteins may also be toxic to the cell or disrupt normal homeostasis by addition of new catalytic reactions. Lack of activity could be explained as proteins could be insoluble or missing a posttranslational modification present in the original host. The control would not account for protein functionality as natural VanAB activity would be induced by

vanillate, but the control does show the growth defect. VanAB is proved to be a better option for engineering the conversion of syringate into gallate in KT2440.

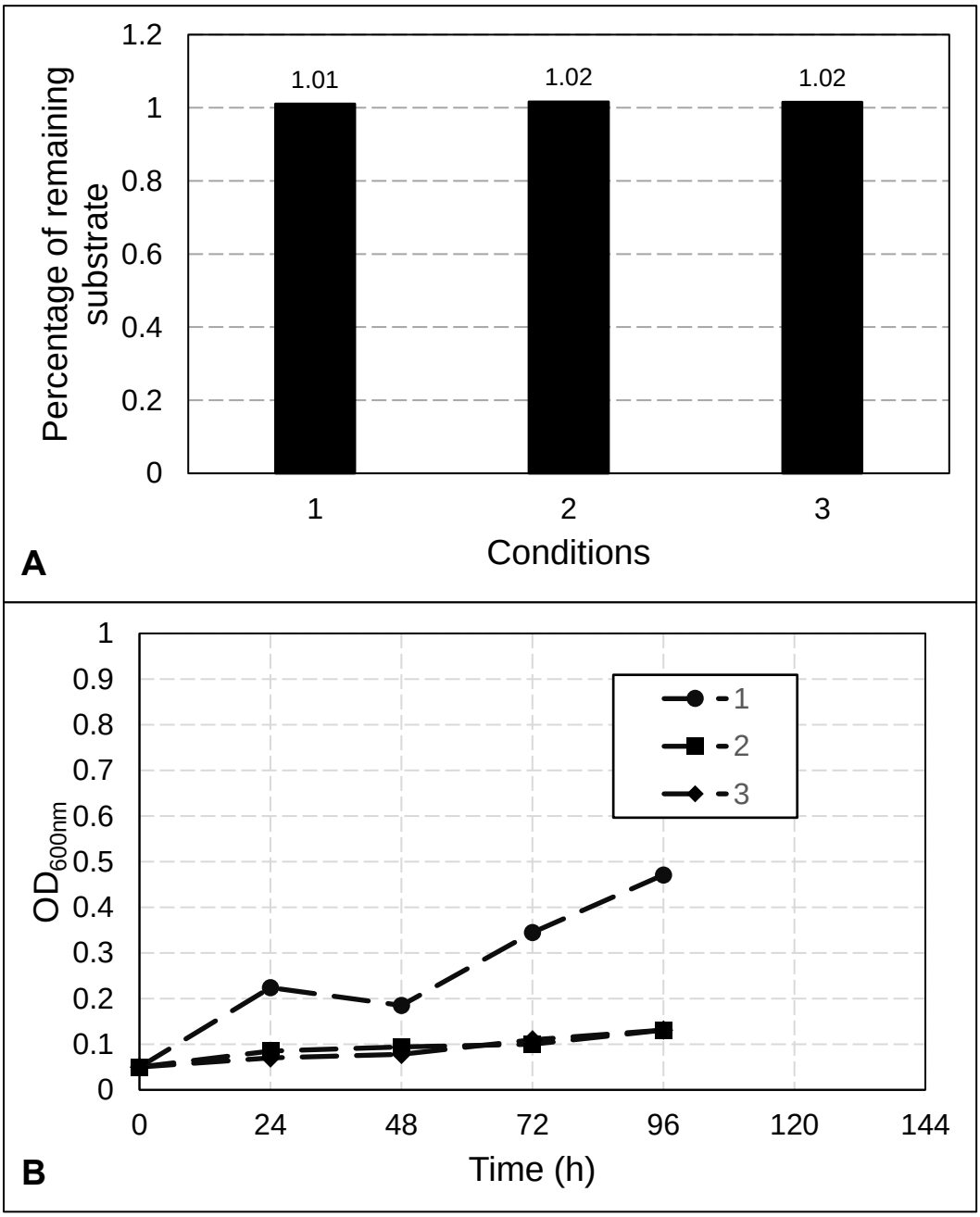

Figure 2-6. Syringate utilization. Grown in M9 minimal media containing 0.25% (w/v) syringate. Utilization was monitored for 96 h via ^{1}H NMR. Conditions: 1, blank media; 2, KT2440 with empty pBBR vector; 3, KT2440 with pBBR-desA-ligM. A, percentage of remaining syringate B: OD_{600nm}. Experiment was done in single trial.

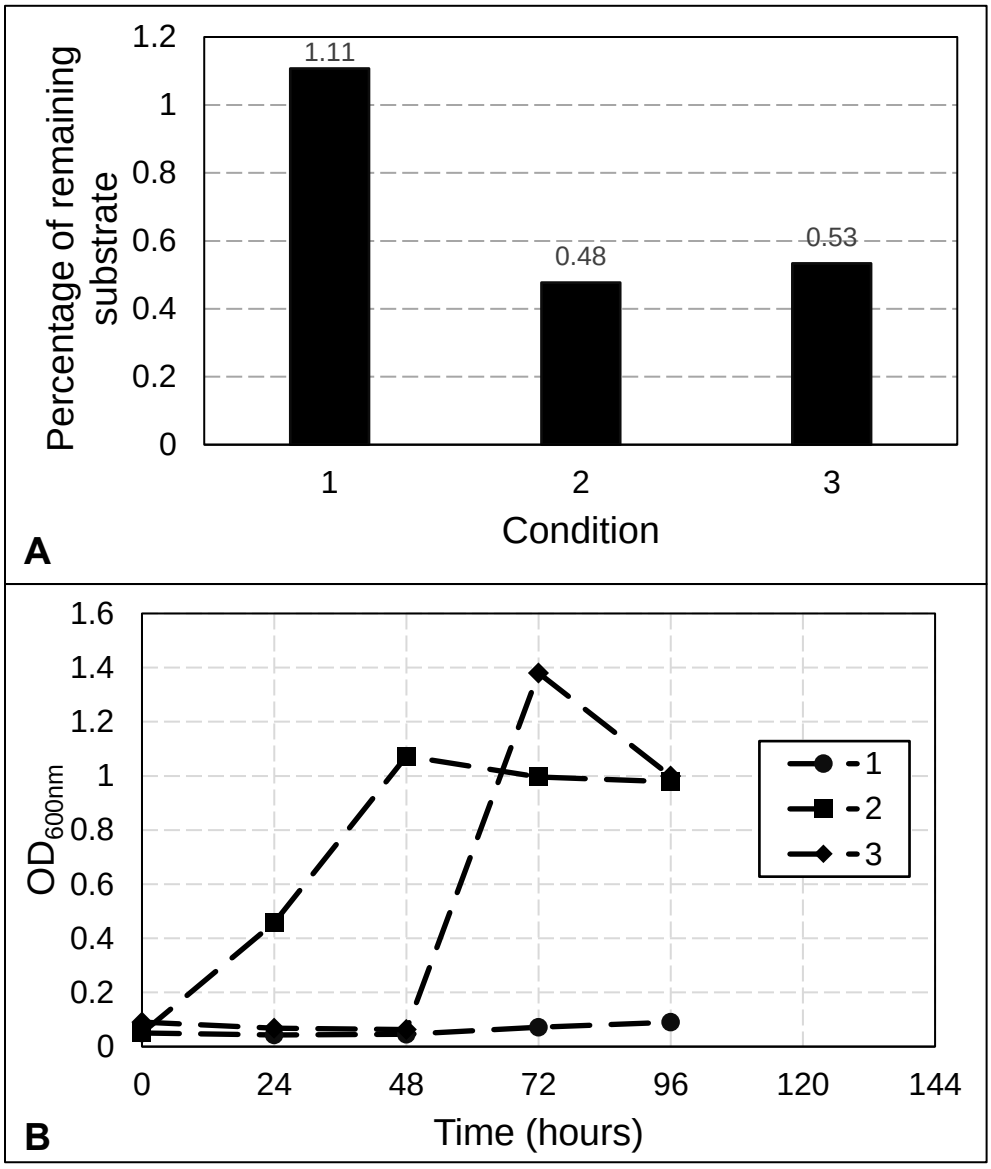

Figure 2-7. Vanillate utilization. Grown in M9 minimal media containing 0.25% (w/v) vanillate. Utilization was monitored for 96 h via ^{1}H NMR. Condition 1, blank media; 2, KT2440 with empty pBBR vector; 3, KT2440 with pBBR-desA-ligM. Experiment was done in single trial.

The plasmid expression the FerA, LigV, and FerB enzymes was transformed into KT2440 and the conversion from sinapate to syringate was monitored. Degradation of sinapate was apparent with all three culture conditions, but syringate was only formed in the strain transformed with the plasmid (Fig. 2-8). Since the produced syringate cannot be

consumed by KT2440 naturally, its concentration increased continuously. The expression of the *ferA-ligV-ferB* construct is proved to be sufficient for the conversion of sinapate to syringate in KT2440. In conjunction with the endogenous VanAB enzyme, the FerA-LigV-FerB enzymes should enable KT2440 to metabolize sinapate and syringate, which are derivatives of S-lignin. Future experiments should be conducted to test this hypothesis. Unlike ferulate and coumarate, the further metabolism of sinapate and syringate can serve as the carbon source for growth in adipate production.

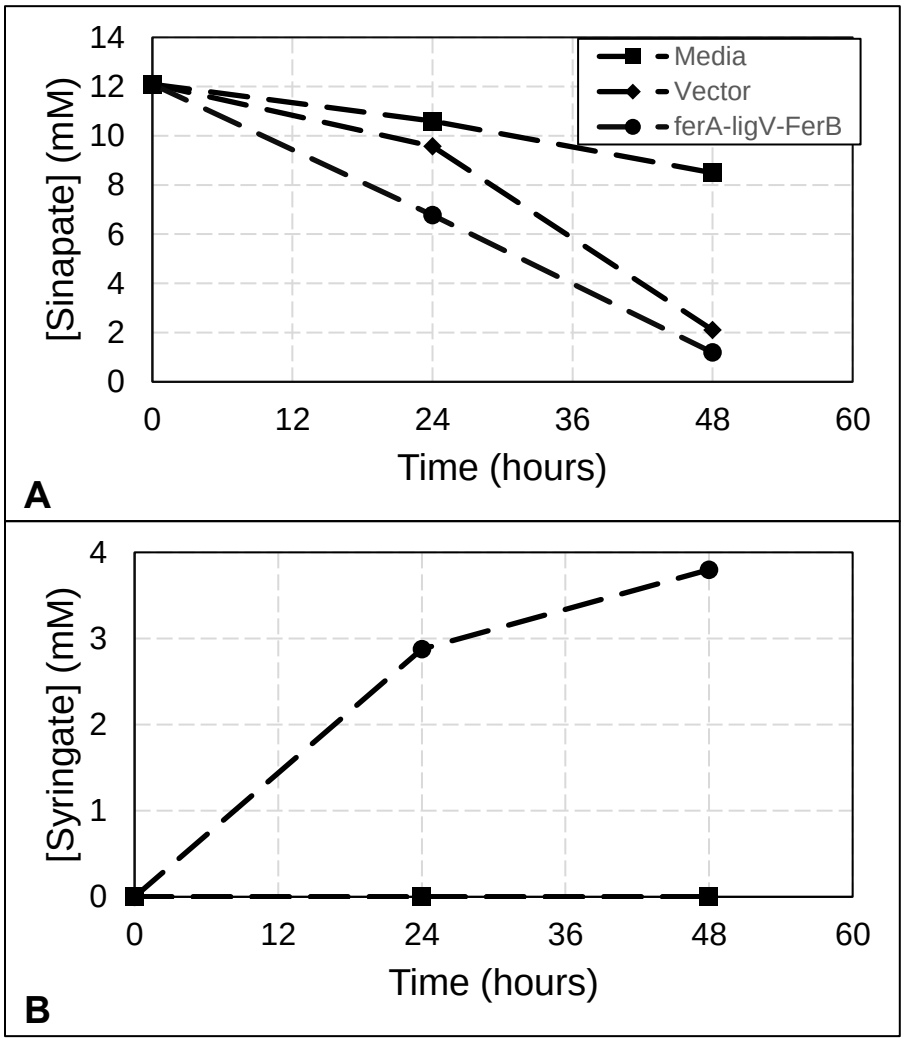

Figure 2-8. Sinapate utilization by KT2440 transformed with ferA-ligV-ferB plasmid. Grown in M9 minimal media containing 0.25% (w/v) sinapate. Utilization was monitored via ^{1}H NMR. Vector is KT2440 transformed with an empty pBBR vector. A, sinapate utilization; B, syringate production. Experiment was done in single trial.

CHAPTER 3 - Engineering *Pseudomonas putida* KT2440 for the Synthesis of Adipic Acid from Lignin-derived Aromatics

3.1 Synthetic pathway for adipate production in *P. putida* KT2440

We envision an engineered strain of KT2440 that has the ability to utilize all parts of depolymerized lignin and to convert it to adipate or biomass to sustain cellular growth and function. Such a process will convert a renewable resource that is seen as a waste product into adipate. The starting material for this process would avoid the toxicity and non-sustainability issues of current industrial synthesis. A pathway converting β-ketoadipate into adipate will be expressed in the strain. This conversion is reported using *E. coli* phenyl acetic acid degradation (*paa)* enzymes PaaH and PaaF and a trans-enoyl-CoA reductase (TER) from *Treponema denticola* (TdTER).[31] These enzymes, with the help of endogenous thiotranferase activity, convert β -ketoadipoyl-CoA into adipate (Fig. 3-1). Furthermore, *P. putida*'s β-ketoadipate pathway will be engineered to stop at β-ketoadipoyl-CoA, which will then be funneled into our non-natural biosynthetic pathway. The activation of β-ketoadipate into β-ketoadipoyl-CoA is catalyzed by an enzyme encoded by *pcaIJ*, which is part of the β-ketoadipate pathway. Deletions of *pcaF* and *paaJ* will help prevent the degradation of pathway intermediate, β-ketoadipoyl-CoA, into succinyl-CoA and acetyl-CoA.

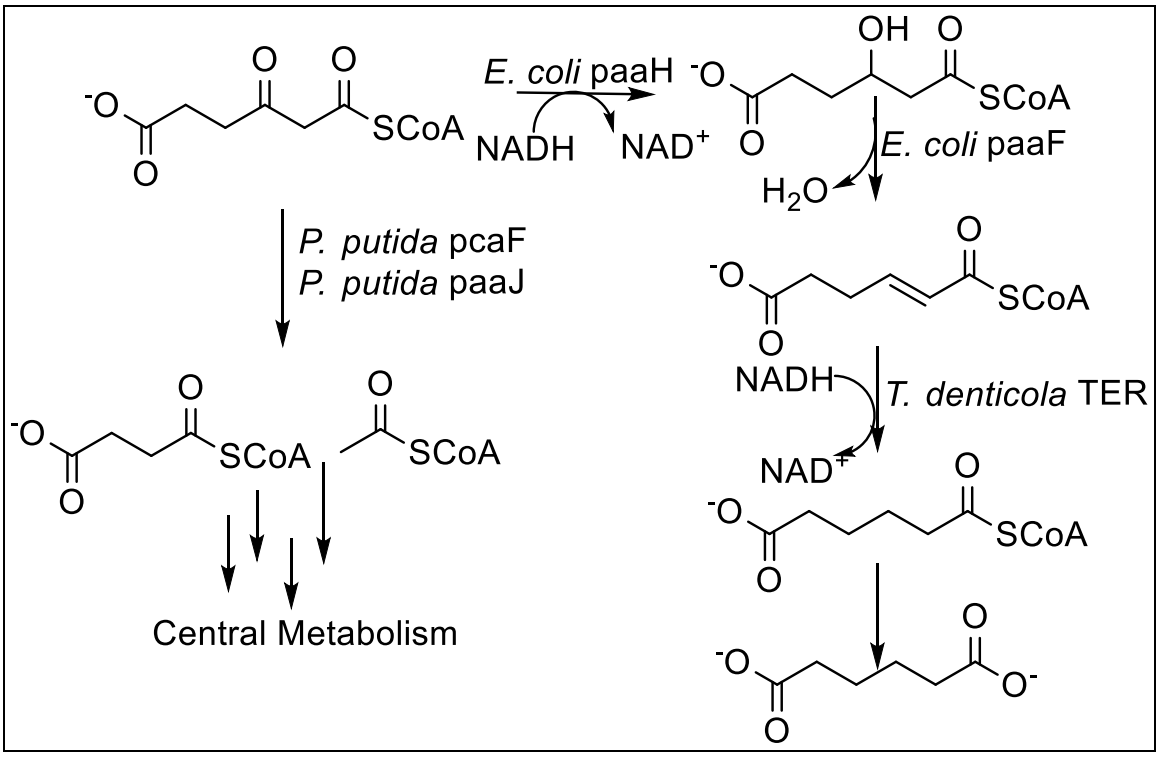

Figure 3-1. Biosynthetic pathway for adipate. Non-natural biosynthetic pathway that converts β-adipoyl-CoA into adipate via the action of *E. coli* PaaH and PaaF and *T. denticola* TER proteins. Deletion of β-ketothiolase, PcaF, prevents carbon flux to biomass and diverts it to the biosynthetic pathway.

3.2 Developing a genetic toolbox for *P. putida* KT2440

In order to develop a genetic toolbox that allows for the fine-tuning of the expression level of enzymes, a promoter library of varied strength and cloning vectors with varied copy number were built. Five promoters, P_{A1}, P_j, P_{tac}, P_n and P_{lac} were cloned in front of sfGFP-encoding gene in a pBBR vector and transformed into *P. putida*. Promoter P_{A1} is from T7 phage, P_{lac} is from the *E. coli* lac operon, and P_{tac} is a hybrid promoter made from tryptophan and lactose promoters. By using promoters with varied strength, enzyme expression can be tuned to an appropriate level. The pBBR vector was chosen because it replicates in *E. coli*, for ease of cloning, and it also replicates in *P. putida*. Fluorescence was read as a proxy for DNA promoter strength as the promoter was

the only variable between expression cassettes. The P_{A1} promoter was determined to be the strongest followed by P_j, P_{tac}, P_n and then P_{lac} (Fig. 3-2).

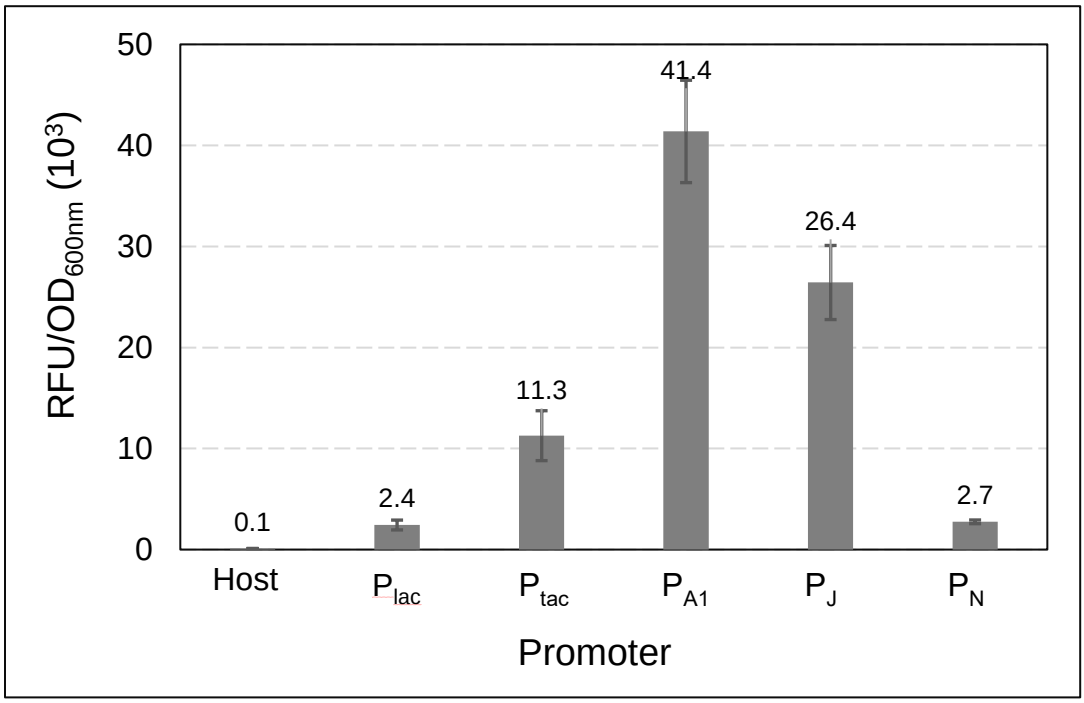

Figure 3-2. Promoter strength experiment. Five promoters were tested for their expression strength using sfGFP as a reporter. The fluorescence values were normalized to cell growth. The data is the average of three measurements. The error bars indicate the standard deviation. RFU, relative fluorescence units.

pBBR, pSEVA651, and pSEVA621 plasmids with pBBR, RK2, and RFS1010 replication origins, respectively, were tested for cellular copy numbers in *P. putida* KT2440 strain. Using sfGFP as a reporter, the relative copy numbers of RK2 and RFS1010 to pBBR replication origin were determined with two promoter systems, P_{tac} and P_{A1}. The results using the two promoters are in good agreement. The relative ratio of pBBR:RK2:RFS1010 replication origins is 20:2:5 (Fig. 3-3).

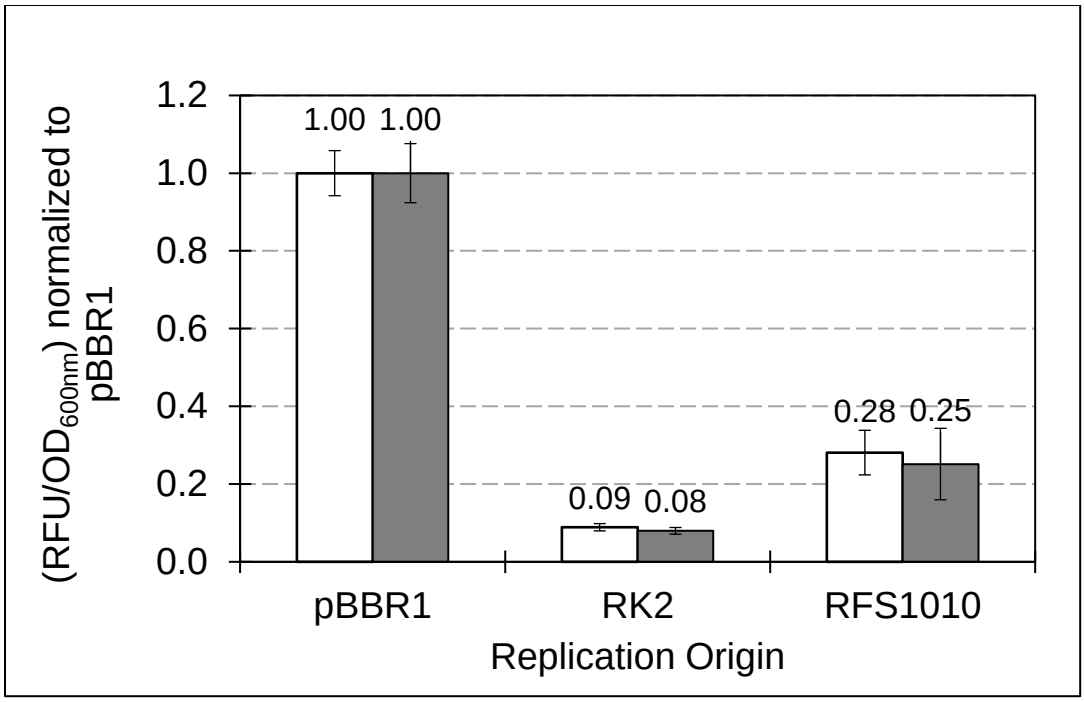

Figure 3-3. Relative plasmid copy number experiment. Plasmid copy number was determined for pBBR1, RK2, and RFS1010 replication origin with two differing promoters, P_{tac}, white bars, and P_{A1}, grey bars.The data is the average of three measurements. The error bars indicate the standard deviation. RFU, relative fluorescence units.

3.3 Minimizing the metabolism of β-ketoadipate

A ΔpcaF strain of *P. putida* KT2440 was generated via homologous recombination. Deletion of this gene should lead to over accumulation of β-ketoadipoyl-CoA. When this strain was cultured on coumarate and ferulate as the sole carbon sources, a prolonged lag phase was observed. However, the deletion of *pcaF* was insufficient to prevent cell growth on the two aromatic compounds (Fig. 3-4). Additional enzyme(s) was hypothesized to allow the cell to metabolize 3-ketoadipate. A protein BLAST search of the *P. putida* genome was performed using the PcaF protein as the query sequence. A protein encoded by the *paaJ* gene was found to have a 68% sequence identity and 81% sequence similarity to PcaF. Another protein, which is annotated as PcaF-II, has 41% sequence identity and 57% sequence similarity to PcaF. qPCR experiments performed in

our group demonstrated that the transcription level of *paaJ* gene was significantly upregulated when cells were cultured in 3-ketoadipate, which was not true for the *pcaF*II gene. Based on the qPCR results, the *paaJ* gene was deleted in the wild type KT2440 and the *P. putida* ΔpcaF strains. The strains ΔpaaJ and Δ2 were cultured on coumarate and ferulate as the sole carbon sources (Figure 3-4). Deletion of *pcaF* and *paaJ* increased the lag phase to 72 h on just coumarate and ferulate, providing evidence that carbon flux towards cell biomass was minimized. This also provides the first piece of evidence of crosstalk between two differing aromatic catabolic pathways: the β-ketoadipate pathway and the phenylacetic acid pathways. The same four KT2440 strains were also tested for growth on glucose to screen for any metabolic deficiencies. No difference in growth was observed (Fig. 3-5).

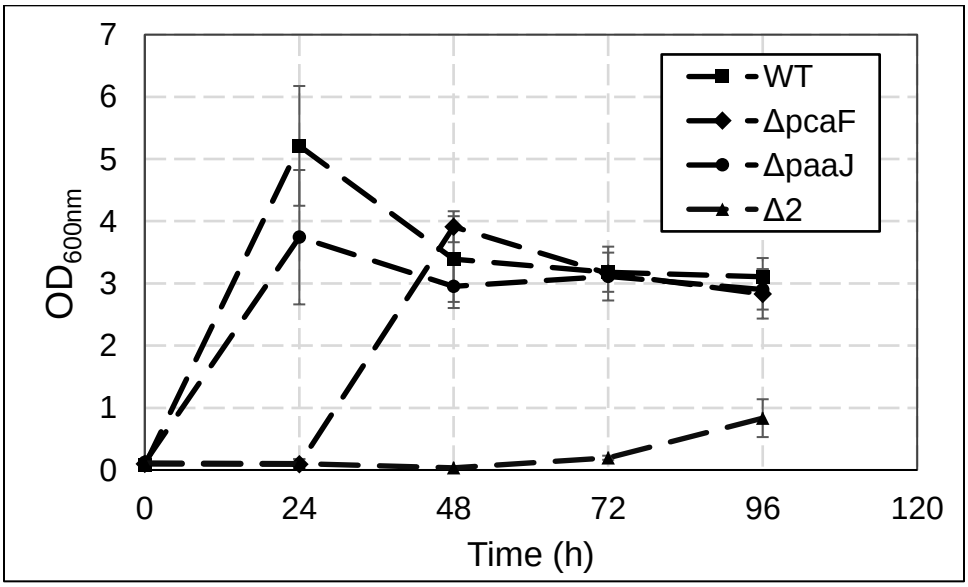

Figure 3-4. Growth of *P. putida* KT2440 mutants. Experiment was conducted in M9 minimal media containing 0.25% (w/v) coumarate and 0.25% (w/v) ferulate as the sole carbon sources.

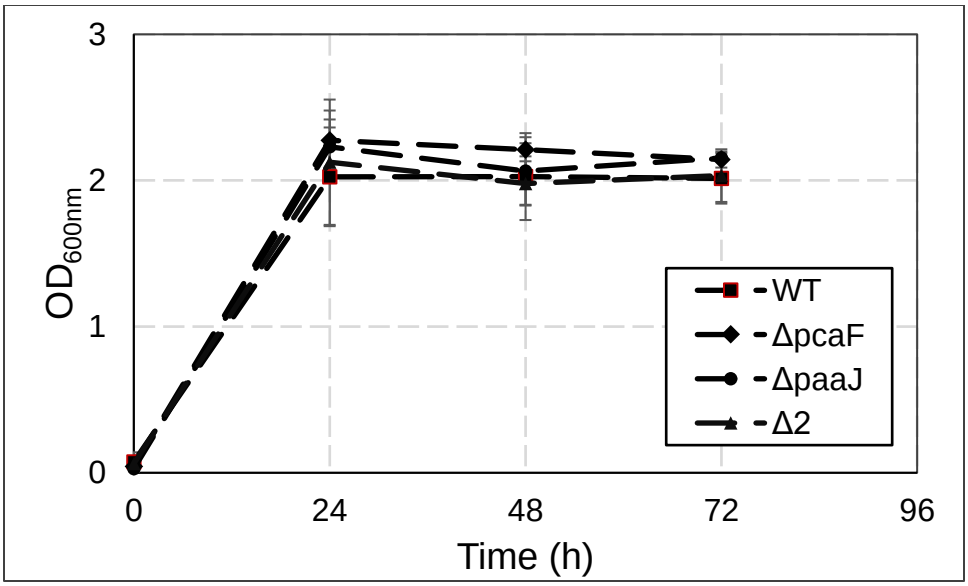

Figure 3-5. Growth of *P. putida* KT2440 mutants in glucose. For this experiment, cells were grown in M9 minimal media with 0.25% (w/v) glucose.

With a strain that is capable of growth on glucose, but has minimal growth on ferulate and coumarate, metabolite accumulation was monitored with ^{1}H NMR when the strain was cultured on 0.25% (w/v) glucose, coumarate, and ferulate. The Δ2 strain led to the highest β-ketoadipate titer following 48 hours of culture (Fig. 3-6). The consumption of carbon sources was also monitored. Strain utilization of coumarate was not different, while the utilization of ferulate was. The Δ2 strain never fully converted all ferulate and vanillate into β-ketoadipate. The ΔpcaF strain consumed vanillate slower than the wild-type and ΔpaaJ strains. The PcaF protein is part of the pathway for vanillate degradation, so an increase in the time to break vanillate is logical (Fig. 3-7).

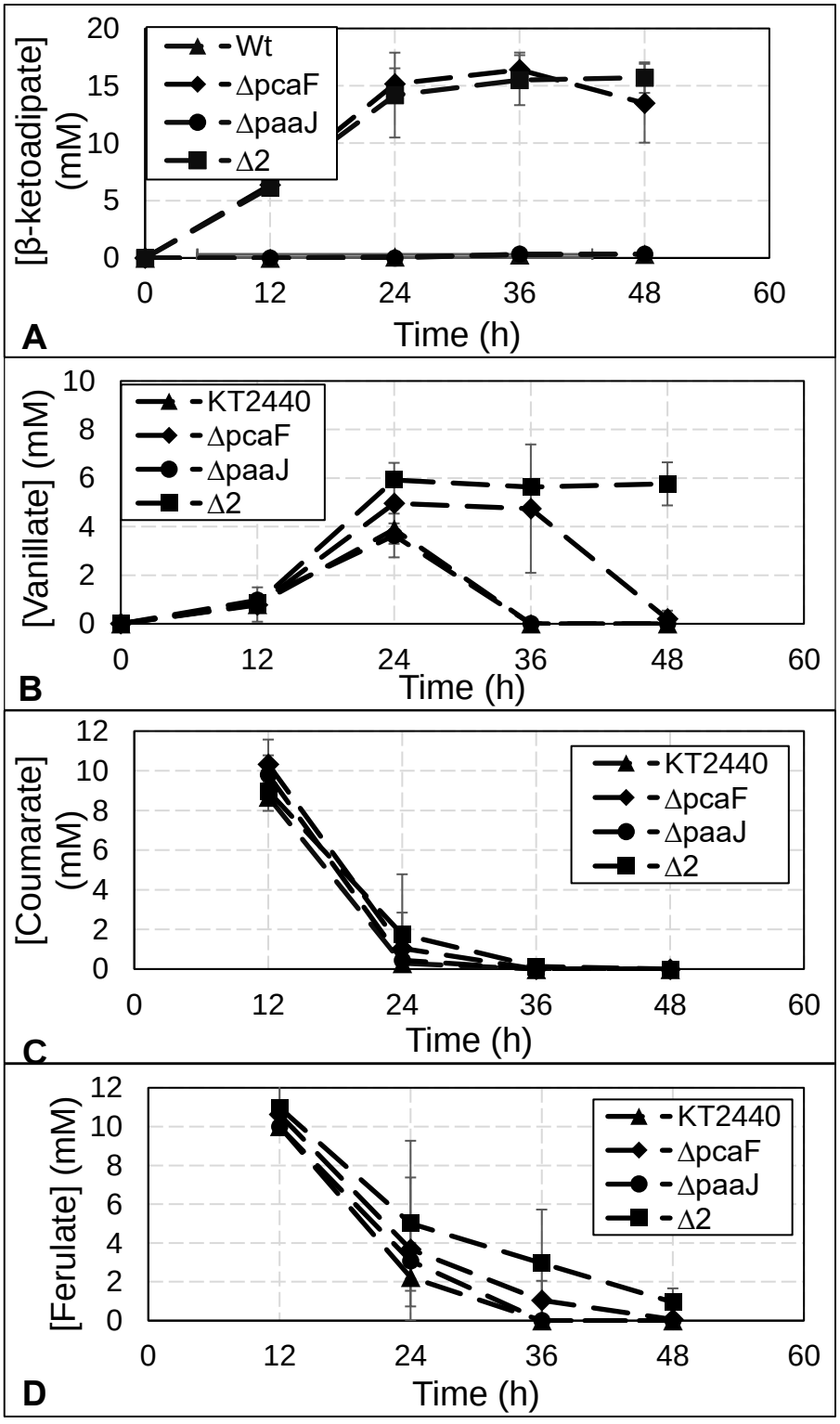

Figure 3-6. Metabolite accumulation experiment. Metabolite accumulation was tested for *P. putida* strains grown on M9 minimal media with 0.25% (w/v) glucose, 0.25% (w/v) ferulate, and 0.25% (w/v) coumarate. The data is the average of three measurements. The

error bars indicate the standard deviation. A, β-ketoadipate accumulation; B, vanillate consumption; C, coumarate consumption; D, ferulate consumption.

3.4 *De novo* biosynthesis of adipate through plasmid-based pathway

Early attempts to analyze metabolite accumulation by High-Performance Liquid Chromatography (HPLC) were complicated by the low resolution of the method. Quantification of metabolites was done using ^{1}H NMR. The β-ketoadipate had been synthesized using a *P. putida* Δ3 catalyst and was purified by a collaborator. Authentic samples of 3-hydroxyadipic acid was prepared by a collaborator by chemical reduction.

It was hypothesized that lower aeration rates would lead to a lower oxygen transfer rate, which would reduce oxidative phosphorylation and increase intracellular levels of reducing equivalents. Our adipate biosynthetic pathway requires reducing equivalents, so an increase in their concentration may help to convert pathway intermediates to adipate. Therefore, at 48 h the cultures were split into half at an aeration rate of 100 rpm and 250 rpm, respectively. Plasmids containing pathway genes in two orientations, PaaFH-TdTer (PT) and TdTer-PaaFH (TP), were transformed into chemical competent cells. Adipate was produced by both strains harboring both plasmids, with the PT plasmid strain out performing the TP plasmid strain. At lower aeration rates, higher adipate titers were achieved. The strain with the PT plasmid produced more 3-hydroxyadipate but there does not seem to be a significant difference in β-ketoadipate levels. The strain with the PT plasmid reached a 3.0% (mole/mole) yield from phenolic starting material at 100 rpm, whereas the strain with the TP plasmid reached only a 0.29% (mole/mole) yield (Fig. 3-7).

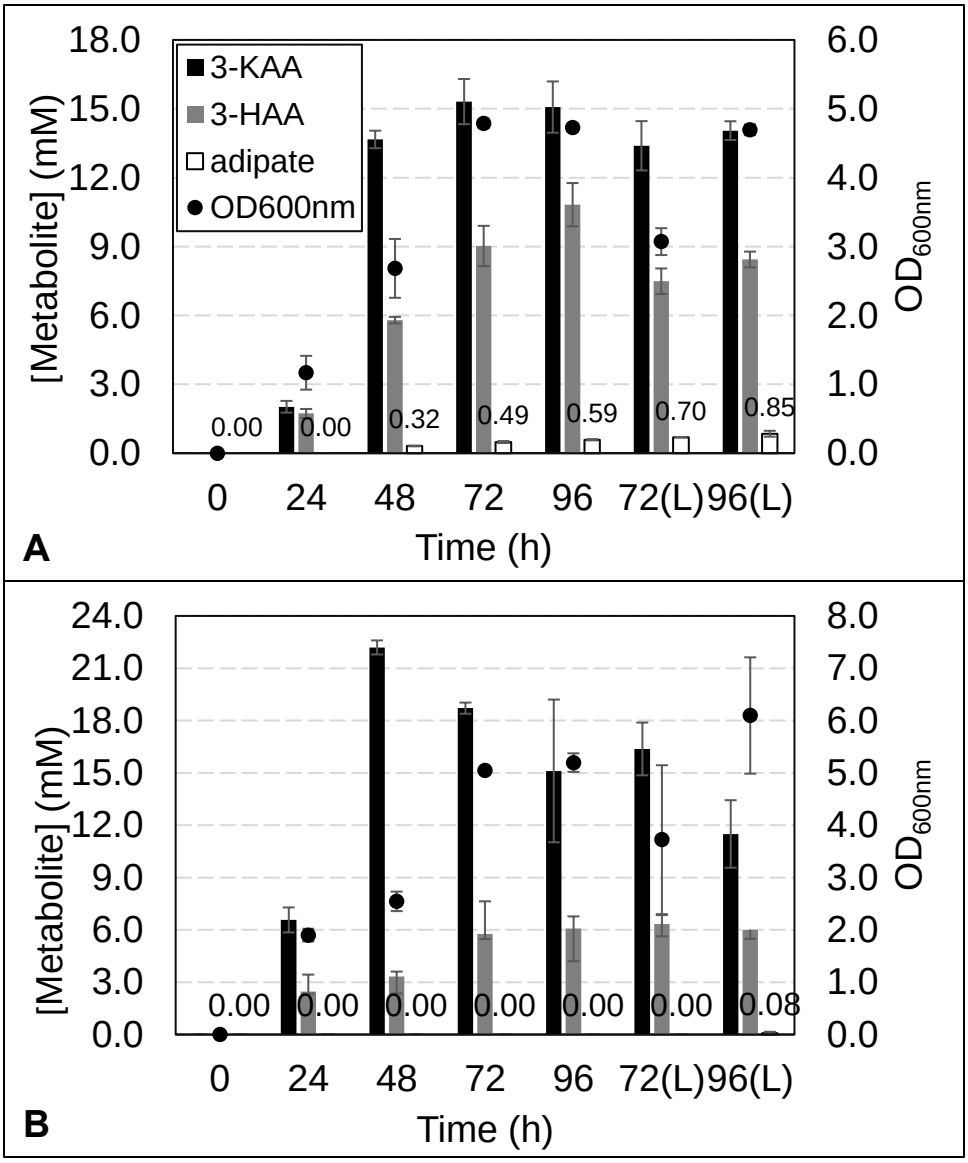

Figure 3-7. Adipate accumulation- plasmid experiment. Adipate accumulation by *P. putida* Δ2 transformed with PT (**A**) and TP plasmids (**B**). Yield of β-ketoadipate, 3-hydroxyadipate and adipate represented by bars; OD_{600nm} of cultures given by dots and left axis. Data labels apply to yield of adipate. Cultures were split at 48 h. Half was aerated at 250 rpm and the other half at 100 rpm (L). Error bars reflect standard deviation, experiment was done in triplicate.

The strain containing the PT plasmid produced more adipate and 3-hydroxyadipate, it consumed phenolic compounds, coumarate and ferulate, slower. At 100 rpm, vanillate was never fully degraded by the strain transformed with the PT plasmid (Fig. 3-9)

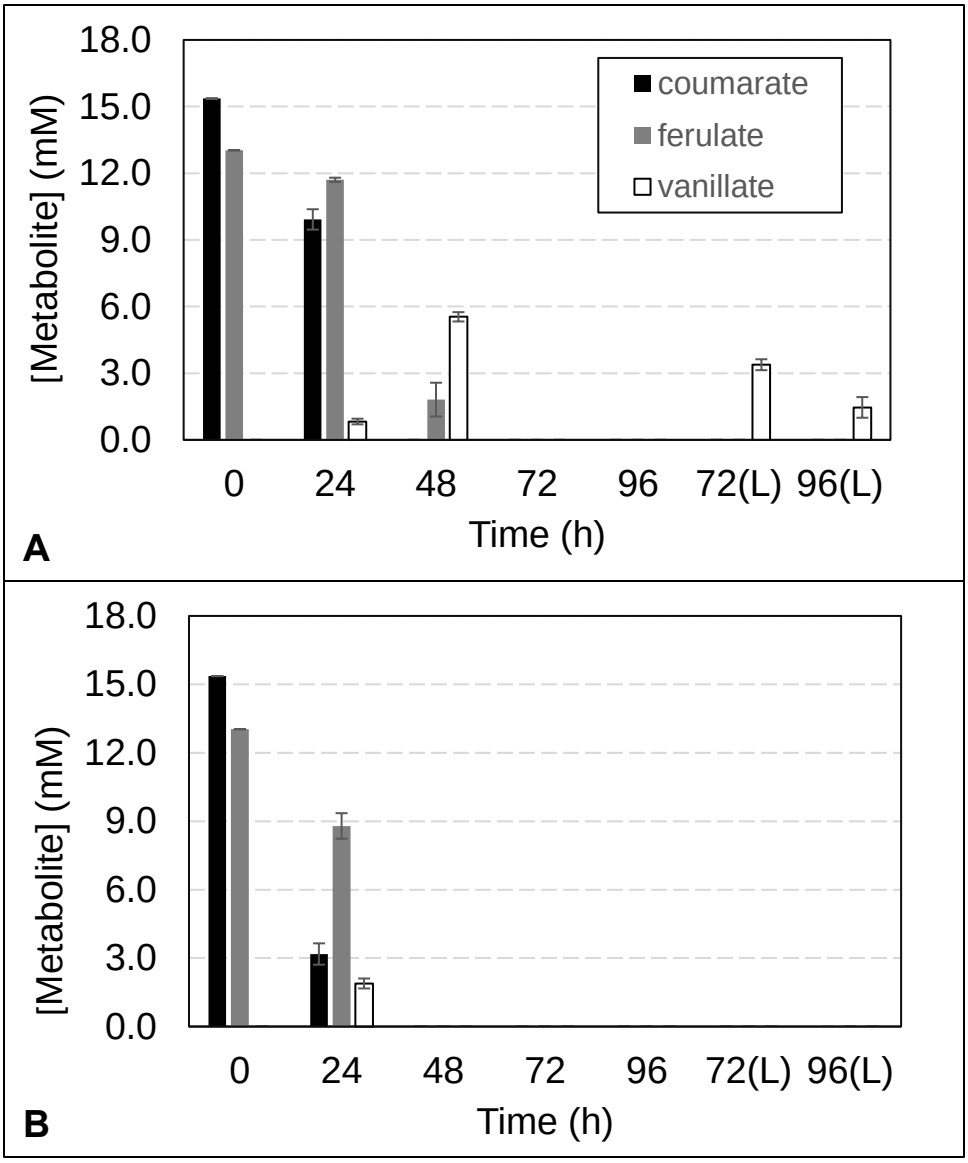

Figure 3-8. Phenolic consumption- plasmid experiment. Phenolic consumption for *P. putida* Δ2 transformed with PT (**A**) and TP plasmids (**B**). Cultures split at 48 hour and half was allowed to shake at 250 rpm and the other half at 100 rpm (L). Error bars reflect standard deviation, experiment done in triplicate.

3.5 Engineering carbon source utilization through the deletion of *crc* gene

The *crc* gene has been shown to play an important role in carbon catabolite repression in *P. putida* KT2440.[32] Catabolite repression is a type of global gene expression regulatory mechanism, which allows microbes to quickly adapt to the available carbon sources by allocating resources in the most efficient manner. We

hypothesized that the deletion of *crc* gene will lead to a strain that can simultaneously convert aromatics into adipate and utilize glucose for cell growth. The *crc* gene was deleted from the wild-type strain and the Δ2 strain to produce the Δcrc and the Δ3 strains, respectively. Together with the two parent strains, the two obtained strains were grown in minimal media containing 0.25% (w/v) glucose, ferulate, and coumarate as the carbon sources. There was no difference in the utilization of ferulate or coumarate. No vanillate was produced as an intermediate in the Δ3 strain, but similar levels were produced by the other three strains. (Fig. 3-9). The data does not support the hypothesis that removal of Crc regulation increases the expression of aromatics utilization enzymes and can lead to the co-metabolism of glucose and aromatic compounds. It indicates that more complex regulatory mechanism(s) may exist. Although the results show no significant improvements in carbon source co-utilization, the Δ3 host was able to consume all coumarate and ferulate, while the Δ2 host never fully converted ferulic acid and vanillic acid into β-ketoadipate. Therefore, the Δ3 host was used to produce β-ketoadipate.

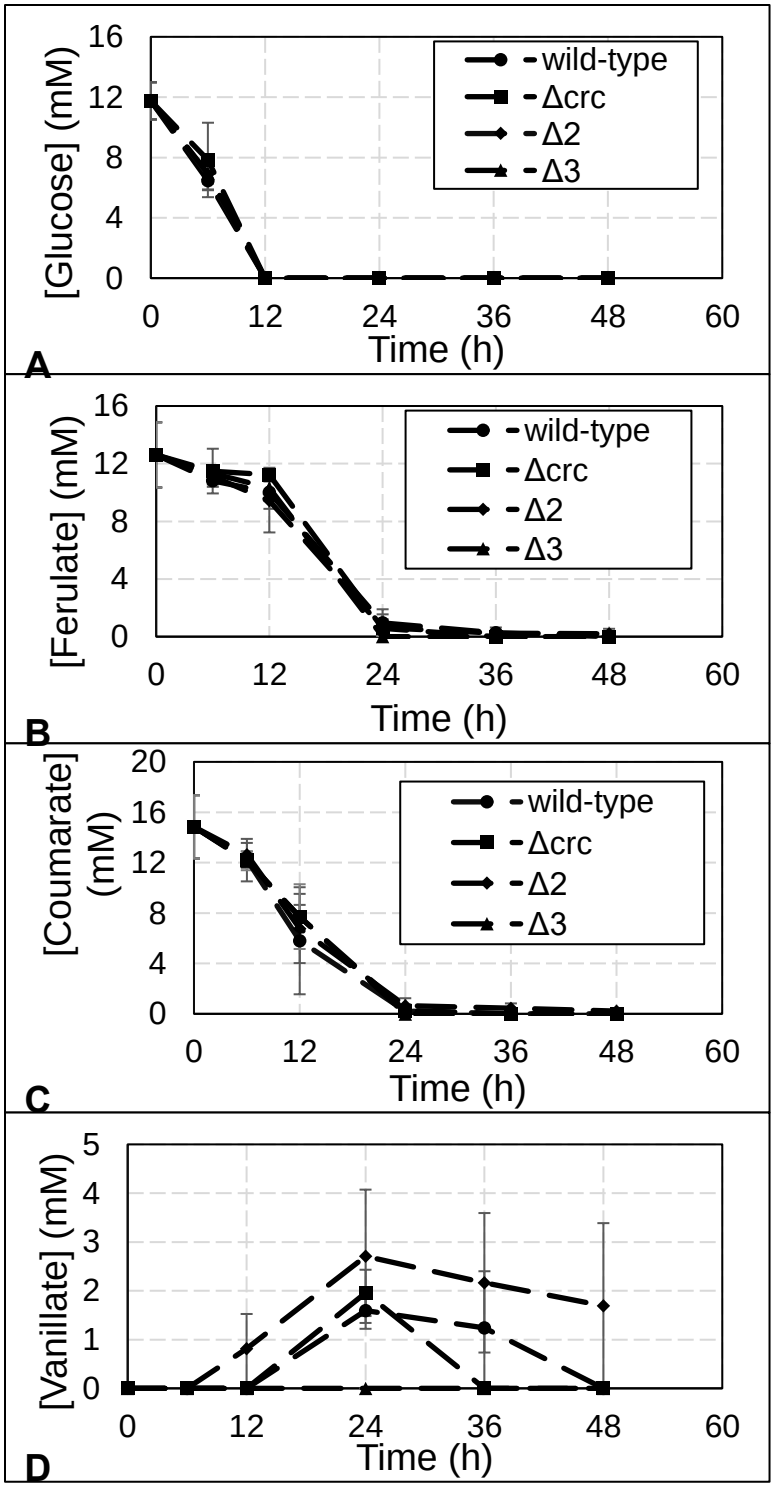

Figure 3-9. Growth test of *crc* deletion strains. The two Δcrc (Δcrc, Δ3) strains and their parents (wild-type and Δ2) were grown in minimal media containing 0.25% (w/v) glucose, ferulate, and coumarate was monitored via ^{1}H NMR for consumption of carbon sources (A, glucose; B, ferulate; C, coumarate; and D, vanillate). Experiments were completed in triplicate where error bars represent the standard deviation.

3.6 *De novo* biosynthesis of adipate through chromosomal integrated pathway

Pathway genes were inserted into the *P. putida* genome using a suicide vector designed for homologous recombination at the *pcaF* gene locus. Pathway integration experiments only investigated the integration of pathway genes in the same order as that of the PT plasmid. By inserting pathway enzymes metabolic burden and inconsistencies assiocated with plasmid-based pathway expression are avoided. Integration also leads to the deletion of the *pcaF* gene. Created mutants were screened using PCR, while the correct genotype was confirmed by DNA sequencing.

A gene cassette, P_{tac}-*paaFH-Tdter*, was integrated into the *pcaF* locus of the wild-type KT2440 to obtain ΔpcaF:: P_{tac}-*paaFH-Tdter*. Then a ΔpaaJ strain was obtained by deleting *paaJ* from the insertion strain to generate *P. putida* ΔpcaF,paaJ :: P_{tac}-*paaFH-Tdter*. The first strain, ΔpcaF:: P_{tac}-*paaFH-Tdter*, was grown on 0.25% (w/v) coumarate, ferulate, and glucose and the highest adipate titer was obtained with a 5.9% (mole/mole) yield. After 48 hours, consumption of β-ketoadipate is observed and after 72 hours, consumption of 3-hydroxyadipate and adipate are also observed. Both insertion strains were examined for adipate accumulation. Strains were grown in M9 minimal media containing 0.25% (w/v) glucose, ferulate, and coumarate. Cells were cultured for 48 h then additional 0.25% glucose was added. Cultures were split in half, then cultured at 250 rpm and 100 rpm respectively. Time points were taken every 24 h. For the ΔpcaF:: P_{tac}-*paaFH-Tdter* strain, consumption of intermediates was apparent, but ameliorated at 100 rpm. This strain yielded 9.5% (mole/mole) adipate from phenolics at 100 rpm (Fig. 3-11).

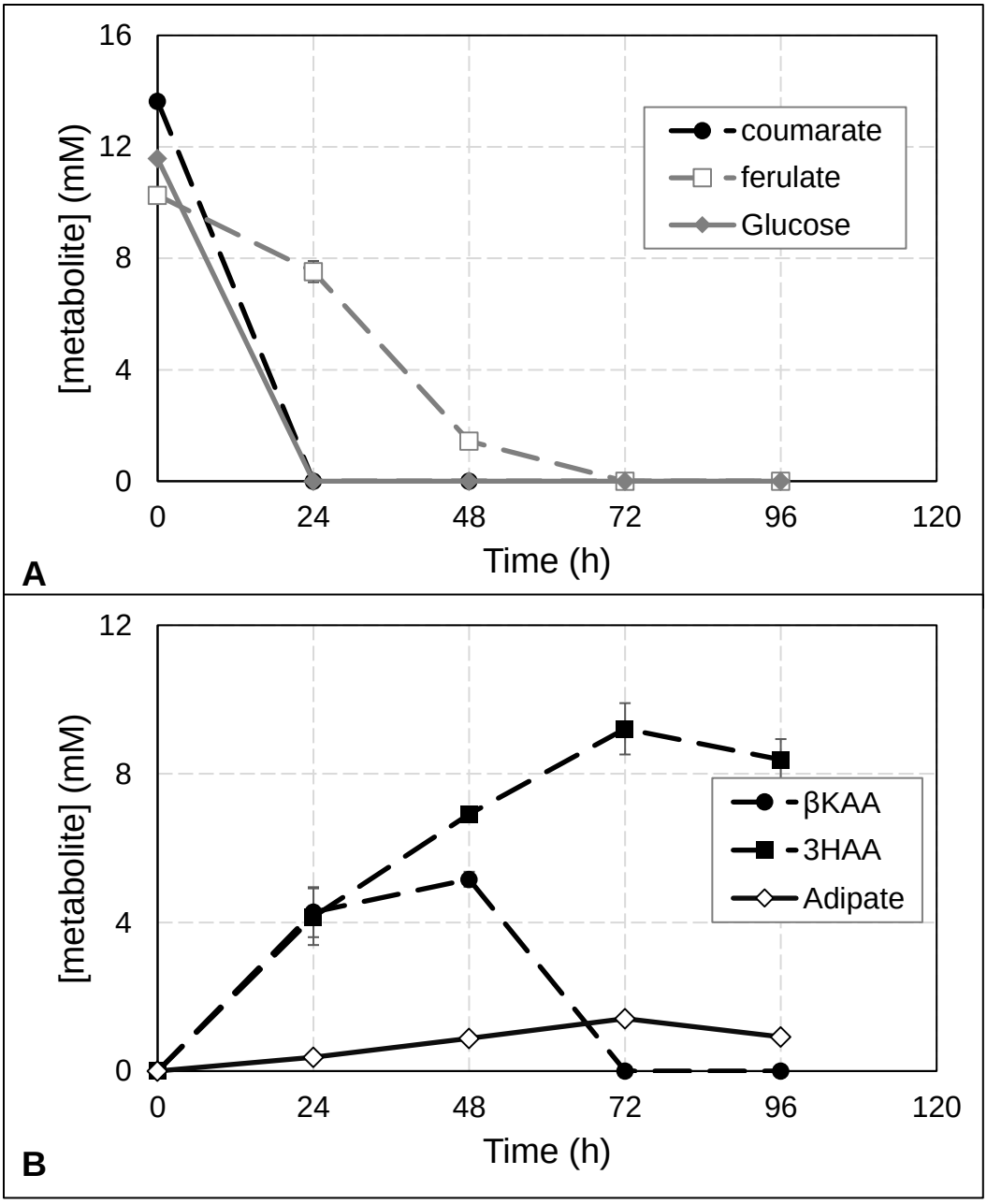

Figure 3-10. Testing of ΔpcaF- P_{tac}-*paaFH-tdter* insertion. P_{tac}-PaaFH was inserted into *P. putida* wild-type, resulting in a *P. putida* ΔpcaF ::P_{tac}-PaaFH-TdTer strain.The metabolite accumulation in 0.25% coumarate and ferulate was monitored. Carbon source consumption (B) and intermediate production (A) are shown. Results reflect an average of triplicate with error bars representing the standard deviation.

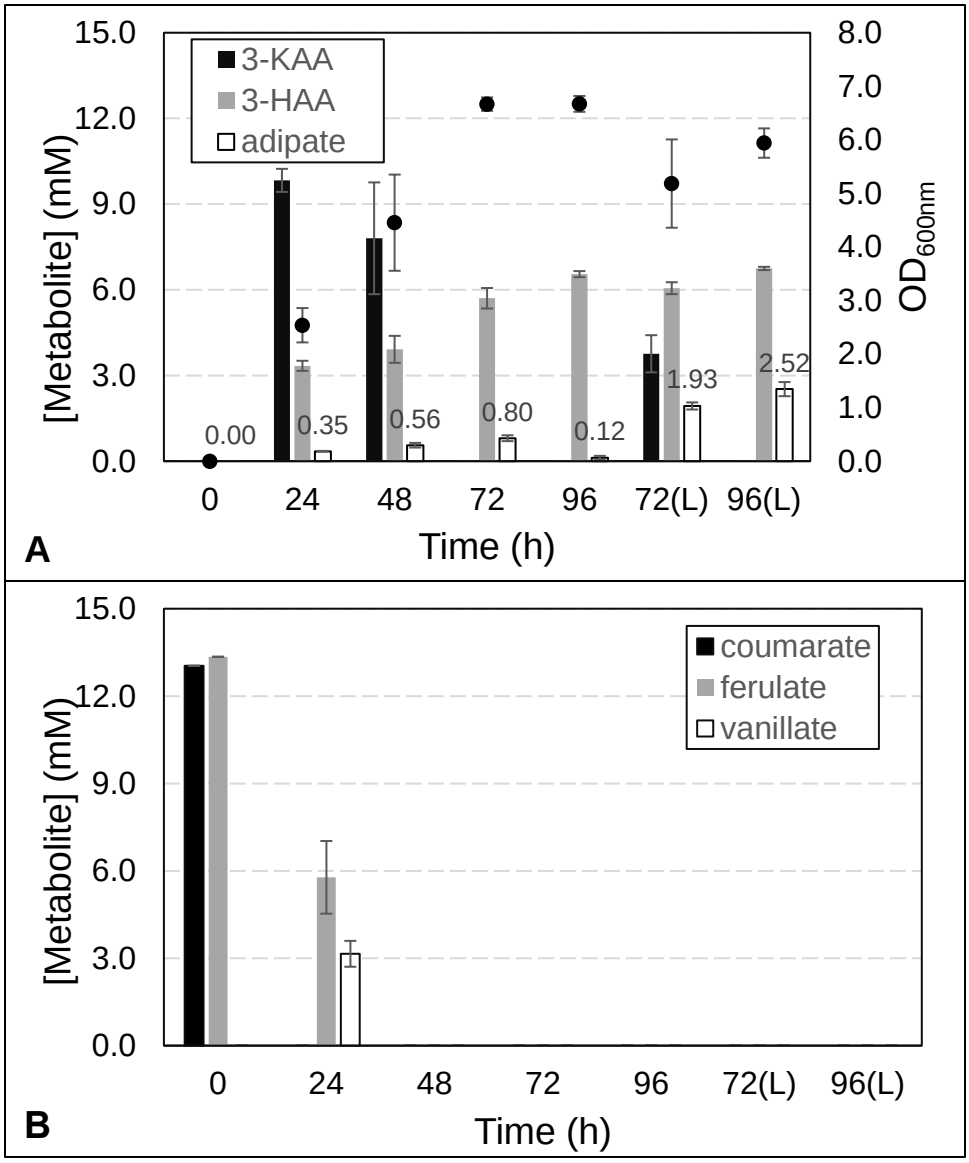

Figure 3-11. Adipate biosynthesis experiment with *P. putida* ΔpcaF ::P_{tac}-*paaFH-Tdter*. Experiment was done in triplicate with error bars representing the standard deviation. Data labels indicate the titer of adipate in mM. Dots represent values of OD_{600nm}. Results from experiments at 100 rpm is denoted by L. A, pathway intermediate biosynthesis; B, phenolic consumption. 3KAA, β-ketoadipate; 3HAA, 3-hydroxyadipic acid.

The Δ2::P_{tac}-*paaFH-tdter* stain accumulation adipate at the highest concentration of 1.52 mM with a yield of 5.7% (mole/mole) from phenolics. This strain did not consume pathway intermediates during the course of the experiments, which is different from the

behavior of ΔpcaF:: P_{tac}-*paaFH-tdter* strain (Fig. 3-12). Both strains achieved higher production of adipate when they were cultured at 100 rpm.

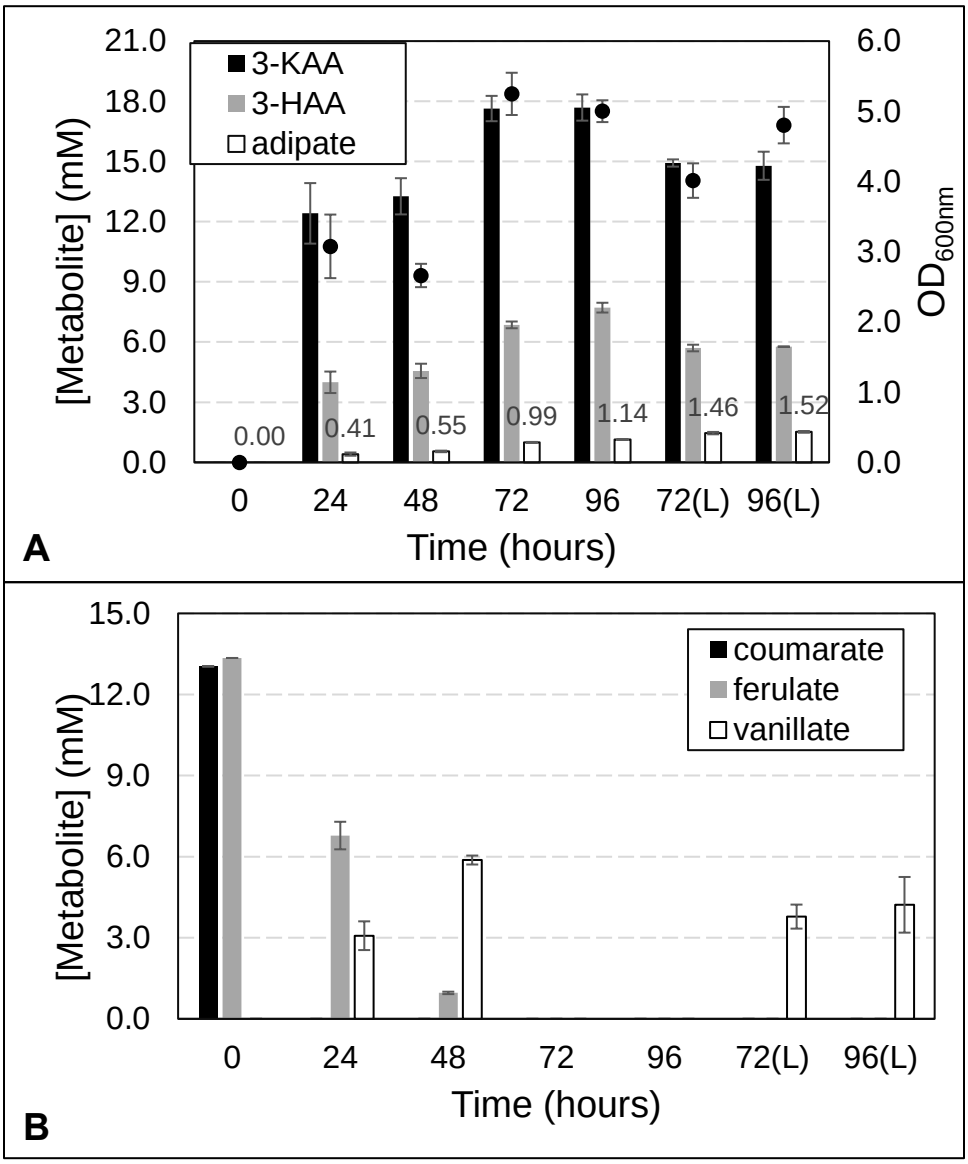

Figure 3-12. Adipate biosynthesis experiment with *P. putida* ΔpcaF,paaJ ::P_{tac}-*paaFH-Tdter*. Experiment was done in triplicate with error bars representing the standard deviation. Data labels indicate the titer of adipate in mM. Dots represent values of OD_{600nm}. Results from experiments at 100 rpm is denoted by L. A, pathway intermediate biosynthesis; B, phenolic consumption. 3KAA, β-ketoadipate; 3HAA, 3-hydroxyadipic acid.

Future experiments will focus on incorporating an additional copy of pathway genes to help convert intermediates towards adipic acid production. Additional enzymes

may be screened for better activity than PaaF and PaaH. To our knowledge, this is the first conversion of lignin-derived aromatics into adipic acid using a cellular biocatalyst. Our currently low conversion poses a problem for purification, as separating pathway intermediates from each other is difficult. Process yield must be increased before industrial production is feasible.

CHAPTER 4 - Materials and Methods

4.1 General methods

^{1}H NMR analysis

Cell culture was centrifuged for five minutes at 21,300 rpm. Supernatant was used directly for quantification. For sample preparation, 450 µL supernatant was combined with 50 µL D_2O with 0.75% (w/v) sodium salt of 3-(trimethylsilyl)propionic-2,2,3,3-d_4 acid (TSP), sodium salt and mixed by vortexing. Samples were transferred into 7-inch, 5 mm NMR tubes and analyzed using the "watersuppression" protocol on a Burker Avance III-JD 300 MHz NMR. This protocol suppresses the water signal using a mathematical function, which allows the quantification of signals that would be masked by water.

To obtain a calibration curve for the quantification of metabolites, standard samples were created by combining 450 µL of authentic sample with known concentration with 50 µL D_2O with 0.75% (w/v) TSP. For each sample, the signal corresponding to protons in TSP was integrated as 1. Signals of metabolites were also integrated. The obtained integration values were graphed against concentrations of the standard. The slope of the obtained straight line is defined as the response factor, which was used to calculated concentration of metabolites in samples.

Cell culture

Cells were grown on plates with LB and agar supplemented with appropriate antibiotic as needed. Transformation mixtures were plated on solid LB agar plates. Saved plasmids in hosts and genetically engineered strains were plated as glycerol stocks stored

at -80 °C. Plates grown overnight for single colonies for both *E. coli* and *P. putida* strains.

Unless otherwise stated, cell cultures were grown at 37 °C for *E. coli* and 30 °C for *P. putida* KT2440 at 250 rpm. Cultures grown in Luria-Bertani medium (LB) or M9 minimal media.

Colony PCR

A colony PCR is performed to check for insertion of a fragment into a plasmid or to genotype a genetically engineered strain. To perform a colony PCR, a single colony is suspended in 10 µL of sterile H_2O and boiled for ten minutes in a thermocycler. The mixture is then centrifuged at max speed for ten minutes. A colony PCR contains 0.8 µL of the supernatant, 5 µL 2x gTAQ master mix, 4 µL sterile water, and 0.1 µL of primer mix, which contains forward and reverse primer at a concentration of 10 µM each. A colony PCR reaction is performed in a thermocycler programed with appropriate conditions.

Preparation of *P. putida* chemical competent cells and transformation

To prepare chemical competent cells, a 5 mL culture was started using a single colony from a freshly streaked plate in LB media. The cells are cultured overnight. The following morning, this culture was subcultured into fresh LB at a 1% (v/v) ratio and allowed to grow for approximately 2.5 h. Cells were collected by centrifugation at 3500*g* at 4 °C for five minutes. Cells are then resuspended in 2.5 mL cold, sterile 0.1M $MgCl_2$ and incubated on ice for two hours. Cells were collected by centrifugation at 3500*g* at 4 °C for five minutes. Cells were resuspended in 1.5 mL cold, sterile TG buffer (15%

glycerol, 75 mM $CaCl_2$, 6 mM $MgCl_2$) and aliquoted into sterile micro-tubes in 50 µL portion. Chemical competent cells are stored at -80 °C.

Competent cells were removed from -80 °C freezer and thawed on ice. Approximately 10-100 ng of plasmid DNA was added to thawed cell suspension and mixed by tapping the tube. Solution was kept on ice for 30 minutes then heat shocked at 37 °C for two and a half minutes. A 200 µL portion of LB was added to the micro-tube. Cells were shaken at 250 rpm at 30 °C for one hour to recover. Cell suspension was plated on LB agar plates with appropriate antibiotic.

Preparation of *P. putida* electrocompetent cells and electroporation

To prepare electrocompetent cells, a 5 mL culture was started using a single colony from a freshly streaked plate in LB media and allowed to grow overnight. This culture was used to inoculate 5 mL of fresh LB at 1% (v/v) ratio. Cells were then grown for approximately 3.5 h. Cells were collected at 16,000*g* for one minute using 1.5 mL micro-tubes in 1.25 mL portions. Each cell pellet (four in total) was resuspended in 1 mL cold, sterile 10% glycerol, then spun down at 16,000*g* for one minute. The process was repeated twice. Each pellet was resuspended in 250 µL cold, sterile 10% glycerol. Cell resuspension was combined before spinning down for 1 minute at 16,000g. Resulting pellet was resuspended in 60 µL cold, sterile 10% glycerol and used for electroporation.

For electroporation, 500 to 1000 ng of plasmid DNA was added to electrocompetent cells, and mixed by tapping the tube. Solution was transferred to a precooled 2 mm gap cuvette. Electroporation was completed using following settings, 2.5 kV, 200 Ω, and 25 µF. A time constant of between 5.1-5.3 ms was observed consistently. Immediately after shock, cells were resuspended in 1 mL SOC media and transferred to a

glass culture tube to recover at 30 °C for one hour. Cells were plated on LB agar plates containing the appropriate antibiotic.

Media preparation

M9 minimal media was prepared by combining sterile components, including trace minerals (1000x), $MgSO_4$ (1000x), $CaCl_2$ (500x), M9 salts (5x) and carbon sources. Glucose was prepared as 20% (w/v) stock solution. Carbon sources such as vanillate, ferulate, coumarate, sinapate, 3OMG, gallate, and syringate were weighed out into a sterile container using a sterile spatula in a balance that was cleaned with 70% ethanol before use. Their limited solubility prevented preparations of a more concentrated solution. The solid was directly combined with other components of the M9 media. The pH of the media was adjusted to neutral by the addition of NaOH (1M) in an equimolar ratio to the aromatic acids. Glucose and aromatic acids were included at a 0.25% (w/v) concentration. Kanamycin was used at 50 µg/mL; gentamycin was used at 10 µg/mL.

4.2 Methods for expanding the aromatics metabolism capability of *Pseudomonas putida* KT2440

P. putida growth curves

P. putida was streaked out onto LB agar plate. An overnight culture was started in 5 mL of LB from a single colony of the freshly streaked plate. Following the OD_{600nm} measurement, calculations were made to determine how much overnight culture was required to seed a 5 mL of media so the starting OD_{600nm} was 0.05. This volume of overnight culture was collected by centrifugation at 16,000*g* for one minute. The cells were washed with the same volume of sterile M9 salts, then resuspended in 50 µL of M9 salts. Obtained cell suspension was used to inoculate 5 mL of freshly prepared M9

minimal media containing the desirable carbon source. The cell growth was monitored by taking the OD_{600nm} measurement of the culture over an appropriate period of time.

Construction of plasmid expressing VanAB

The gene encoding VanAB was amplified via PCR from the genomic DNA of *P. putida* with homology to the vector built into the primers. The backbone was prepared by restriction digestion with *Nde*I and *Xho*I. Plasmid pET28a-*vanAB* was constructed by sequence and ligation independent cloning (SLIC).[33] Plasmid was screened using colony PCR and sequence confirmed.

Testing the function of VanAB in *E. coli* host

E. coli BL21(DE3) competent cells were transformed with plasmid pET28a-*vanAB*. A single colony was introduced into 5 mL LB containing kanamycin. Cells were cultured overnight. A fresh 35 mL of LB containing kanamycin was inoculated with the overnight culture at 1% (v/v). At an OD_{600nm} of 0.8, the cells were induced with 0.5 mM of isopropyl β-D-1-thiogalactopyranoside (IPTG). Cells were allowed to grow for an additional four hours prior to collection by centrifugation at 5000*g* for 10 minutes. Pellet was washed in 35 mL M9 minimal media containing 1% (w/v) glucose and 0.5 mM IPTG. Pellet was resuspended in the same media, then separated into 5-mL aliquots. Cells were collected by centrifugation at 5000*g*. Cells were resuspended in 5 mL of M9 minimal media containing 1% glucose, 0.5 mM IPTG, and 5 mM of vanillate, 3OMG, or syringate. Samples were taken every hour for ^{1}H NMR analysis.

Testing the function of VanAB in *P. putida* host

VanAB was subcloned into a pBBR vector at the *Nde*I and *Xho*I cut sites for the constitutive expression in KT2440. The obtained pBBR-P_{lac}-*vanAB* plasmid was

transformed into *P. putida* KT2440 chemical competent cells. Within 24 h of plating, a single colony was picked to start a 5 mL overnight culture in LB media containing kanamycin. From the overnight culture, 50 µL was used to inoculate fresh M9 minimal media containing 0.25% (w/v) of syringate. Time points were taken every 24 h and metabolites were analyzed using ^{1}H NMR.

Testing the functions of DesA and LigM in *P. putida* host

A plasmid, pBBR-P_{lac}-*desA-ligM* containing *desA* and *ligM* genes of *N. aromaticivorans* was constructed by our group. Cloned genes were confirmed by DNA sequencing. The pBBR-P_{lac}-*desA-ligM* plasmid was transformed into *P. putida* KT2440 chemical competent cells. Within 24 h of plating, a single colony was picked to start an overnight culture in 5 mL of LB containing kanamycin. A 50 µL portion of the overnight culture was used to inoculate 5 mL of fresh M9 minimal media containing 0.25% (w/v) syringate. Time points were taken every 24 h. Metabolites were analyzed using ^{1}H NMR.

Testing the functions of FerA, LigV, and FerB in *P. putida* host

A plasmid, pSEVA651-P_{lac}-*ferA-ligV-ferB* containing *ferA*, *ligV*, and *ferB* genes of *N. aromaticivorans* was constructed by our group. Cloned genes were confirmed by DNA sequencing. The pSEVA651-P_{lac}-*ferA-ligV-ferB* plasmid was transformed into *P. putida* KT2440 competent cells. Within 24 h of plating, a single colony was picked to start an overnight culture in 5 mL of LB containing kanamycin. A 50 µL portion of the overnight culture was used to inoculate 5 mL of fresh M9 minimal media containing 0.25% (w/v) sinapate. Time points were taken every 24 h. Metabolites were analyzed using ^{1}H NMR .

4.3 Methods for engineering *Pseudomonas putida* KT2440 for the synthesis of adipic acid

Construction and characterization of promoter library

P_N and P_J promoters each was assembled from four oligos via overlapping PCR. To this end, all four oligos were first assembled to form full-length products in five cycles of PCR. The full-length fragment was further amplified using a pair of flanking primers in an additional 30 cycles of PCR. DNA fragments encoding the promoters were inserted into an *Xba*I and *Nhe*I treated pBBR-sfGFP plasmid using SLIC method. Obtained plasmids were confirmed by DNA sequencing. pBBR plasmids containing P_{A1}, P_{tac}, and P_{lac} promoters were constructed by our group.

In order to examine the strength of the promoters, the constructed plasmids were transformed into wild-type *P. putida* KT2440. Overnight cultures with appropriate antibiotic were started from single colonies on fresh transformation plates. Once cultures reached stationary phase in 24 h, 1 mL of cells was collected by centrifugation, washed, then resuspended in an equal volume of sterile M9 salts. Samples were prepared in 96-well plate. The OD_{600nm} and the fluorescence were measured using a platereader. For fluorescence measurement, a 485/20 nm filter for excitation and a 528/20 nm filter for emission were used. Additional settings include: 70% gain and optics read from the top. The normalized fluorescence was calculated by dividing the instrument reading by the OD_{600nm} to account for the difference in cell growth.

Determining the relative plasmid copy number

A DNA fragment containing P_{tac}-sfGFP was released from pBBR-P_{tac}-sfGFP using restriction enzymes *Xba*I and *Hin*dIII. Following purification by DNA gel

electrophoresis, the fragment was ligated into vectors pSEVA621 and pSEVA651, which were treated using the same restriction enzymes, respectively. The resulting plasmids, pSEVA621-P_{tac}-sfGFP and pSEVA651-P_{tac}-sfGFP, were confirmed by restriction enzyme digests. Another two plasmids, pSEVA621-P_{A1}-sfGFP and pSEVA651-P_{A1}-sfGFP were constructed with the same cloning strategy. The DNA fragment containing P_{A1}-sfGFP was released from pBBR-P_{A1}-sfGFP. Vector pSEVA651 has a RK2 replication origin, while vector pSEVA621 has a RFS1010 replication origin.

To determine the relative copy number of replication origins, pBBR, RK2, and RFS1010, corresponding plasmids containing P_{tac}-sfGFP or P_{A1}-sfGFP were transformed into wild-type *P. putida* KT2440. Overnight cultures with appropriate antibiotic were started from single colonies on fresh transformation plates. Once cultures reached stationary phase in 24 h, 1 mL of cells was collected by centrifugation, washed, then resuspended in an equal volume of sterile M9 salts. Samples were prepared in 96-well plate. The OD_{600nm} and the fluorescence were measured using a platereader. For fluorescence measurement, a 485/20 nm filter for excitation and a 528/20 nm filter for emission were used. Additional settings include: 70% gain and optics read from the top. The normalized fluorescence was calculated by dividing the instrument reading by the OD_{600nm} to account for the difference in cell growth. Reported numbers were obtained by dividing normalized fluorescence values of cells containing RK2 or RFS1010 plasmid by normalized fluorescence values of pBBR as the relative copy number to pBBR vector.

Chromosomal modification of *P. putida* KT2440

Chromosomal modifications of KT2440 were made using plasmids that were derived from nonreplicating vector, pK19mobsacB (ATCC 87098), which encodes

levansucrase (SacB) and a kanamycin resistance marker. The recombination plasmids were created by ligating DNA fragments that flank the sites of modification into pK19mobsacB vector. In the cases of chromosomal deletions, the flanking fragments were directly ligated together. In the cases of chromosomal insertions, DNA fragments containing insertion sequences were ligated between the flanking fragments. Flanking fragments were amplified from the genomic DNA of KT2440 by PCR. Recombination plasmids were constructed by SLIC method and confirmed by restriction analysis with two separate pairs of enzymes.

To perform chromosomal modification, a pK19mobsacB-derived plasmid was electroporated into electrocompetent cells of the desirable strain. Cells that survived on LB plate containing kanamycin were screened using colony PCR to confirm the chromosomal insertion of the plasmid and to determine its insertion site. Two candidates, one containing integration into the upstream and one containing integration into the downstream flanking region, were further cultured to release the backbone of pK19mobsacB vector. To this end, cells were first cultured in 5 mL of LB media overnight. A 200 µL portion of overnight culture was then used to seed a 5 mL of modified LB media that contains 6.5% sucrose (w/v) and no NaCl. Following the cultivation for an additional six hours, 50 µL of culture was plated on a LB agar plate and incubated overnight. Individual colonies were replicated on LB agar with kanamycin and LB agar plates. Kanamycin-sensitive colonies were screened for the desirable chromosomal modification by colony PCR. Candidates were cultured for genomic DNA isolation and the desirable genotype was confirmed by DNA sequencing.

Biosyntheses of adipate

Biosyntheses of adipate were carried out using both strains containing pathway-encoding plasmid and strains expressing chromosomally integrated pathway. Strains containing plasmid were constructed by transformation. For integration strains, a fresh plate was streaked from the glycerol stock of the desirable strain. To initiate a biosynthesis experiment, a single colony was introduced into 5 mL of LB media containing desirable antibiotic and cultured overnight. The next morning, the OD_{600nm} of the culture was measured to determine the ratio of inoculation so the initial OD_{600nm} of the fresh culture was 0.05. Based on the calculation, an appropriate volume of the seed was collected by centrifugation at 16,000*g* for 1 minute, resuspended in 50 µL of fresh LB, then introduced into 5 mL of freshly prepared media containing 0.25% (w/v) glucose, ferulate, and coumarate. Cells were cultured at 30 °C at an aeration rate of 250 rpm. Samples were taken at every 24 h to determine the OD_{600nm} and the metabolite accumulation of the culture. Metabolite accumulation was monitored using ^{1}H NMR.

For some adipate biosynthesis experiments, a second round of glucose addition was carried out at 48 h by introducing 50 uL of 20% (w/v) glucose solution. For experiments to explore the effect of aeration on adipate biosynthesis, a single culture was split into halves at 48 h following the addition of glucose. One half was cultured at 250 rpm, while the other half was cultured at 100 rpm.

Appendix I – ^{1}H NMR Spectrum

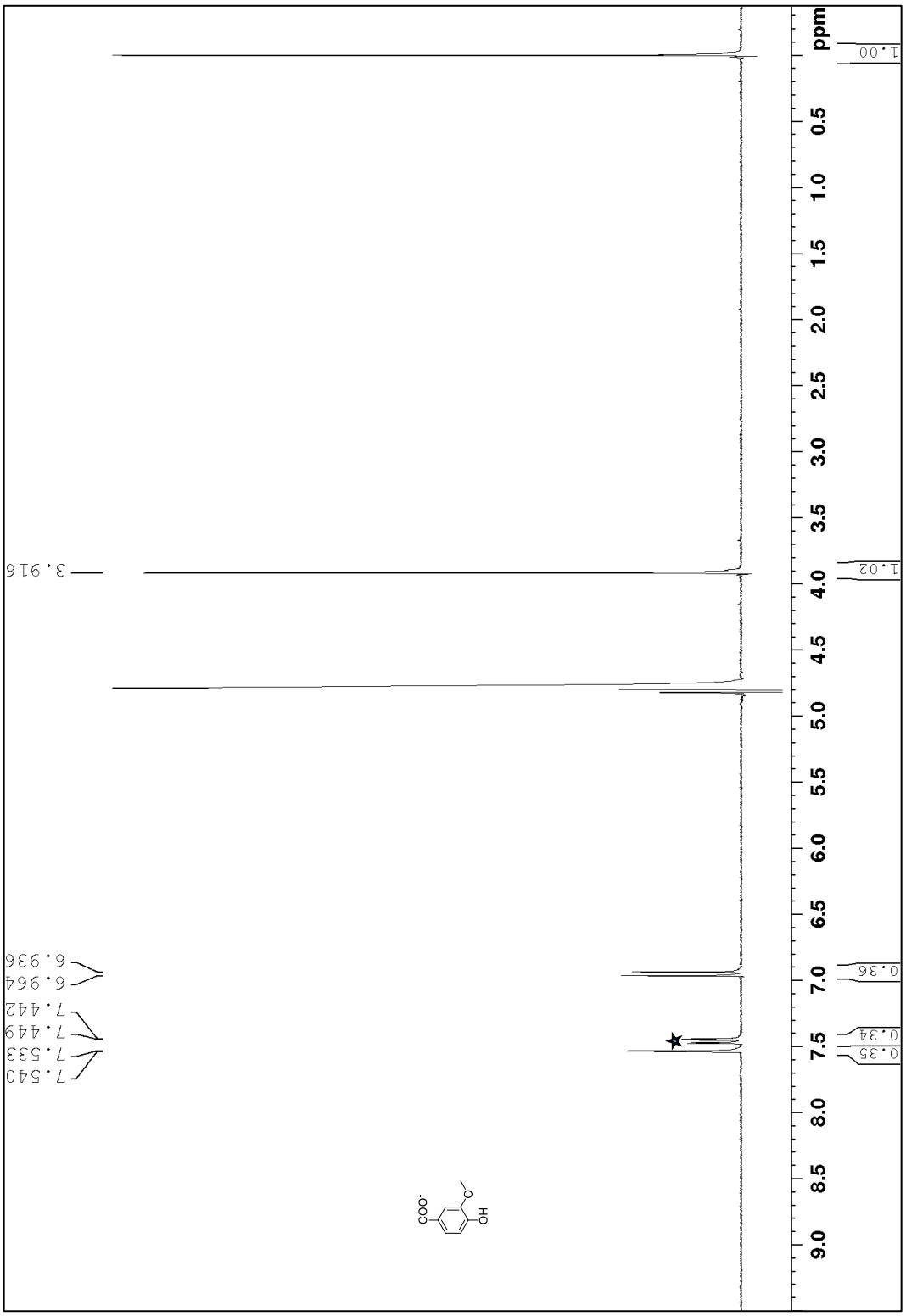

Figure A-1. ^{1}H NMR of vanillate. Vanillate was purchased from Sigma-Aldrich. Signal marked with star was used for quantification, response factor: 42.44 mM/intergration unit.

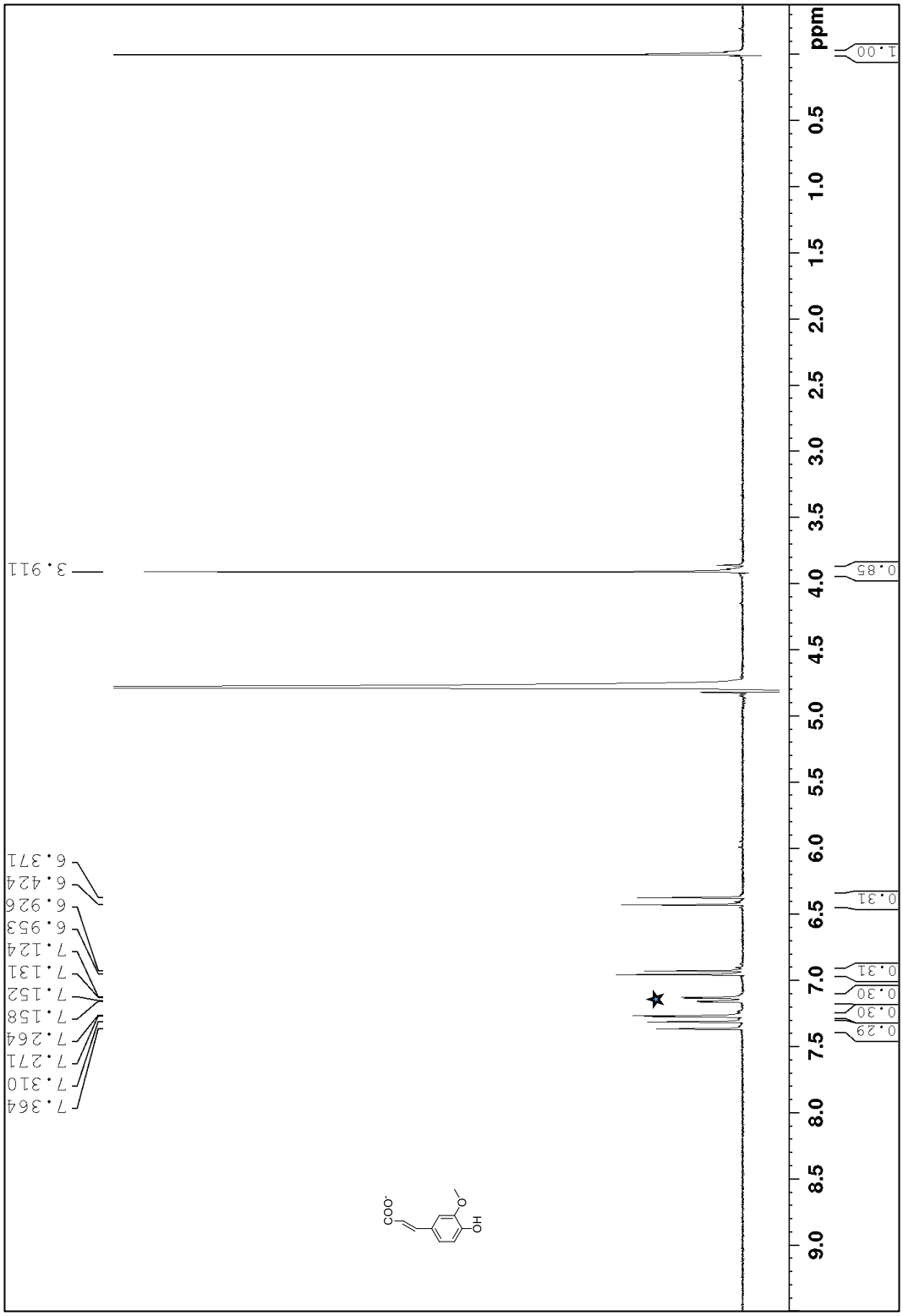

Figure A-2. ^{1}H NMR of ferulate. Ferulate was purchased from Sigma-Aldrich. Signal marked with star was used for quantification, response factor: 39.15 mM/intergration unit.

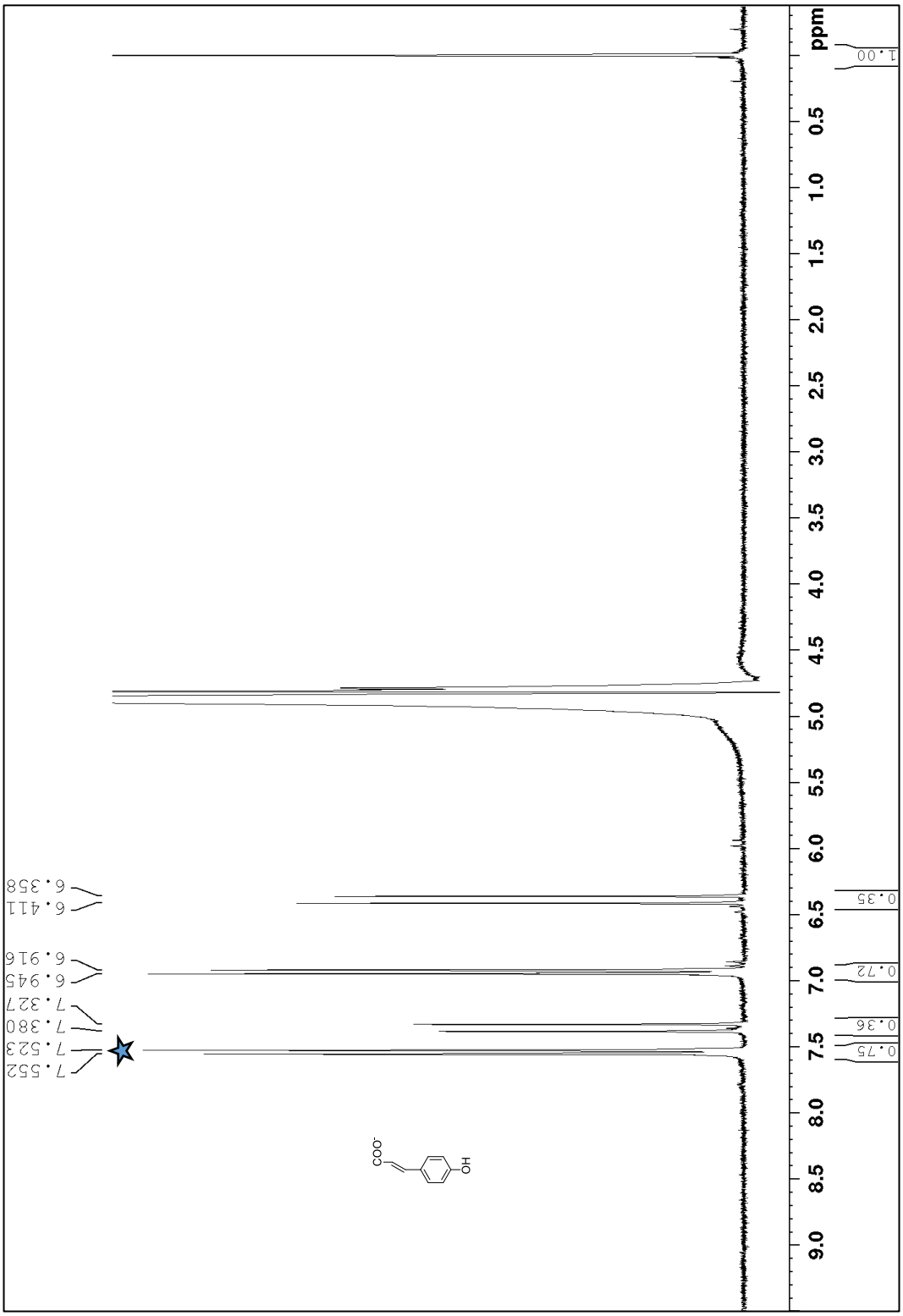

Figure A-3. ^{1}H NMR of coumarate. Coumarate was purchased from Sigma-Aldrich. Signal marked with was star used for quantification, response factor: 19.62 mM/intergration unit.

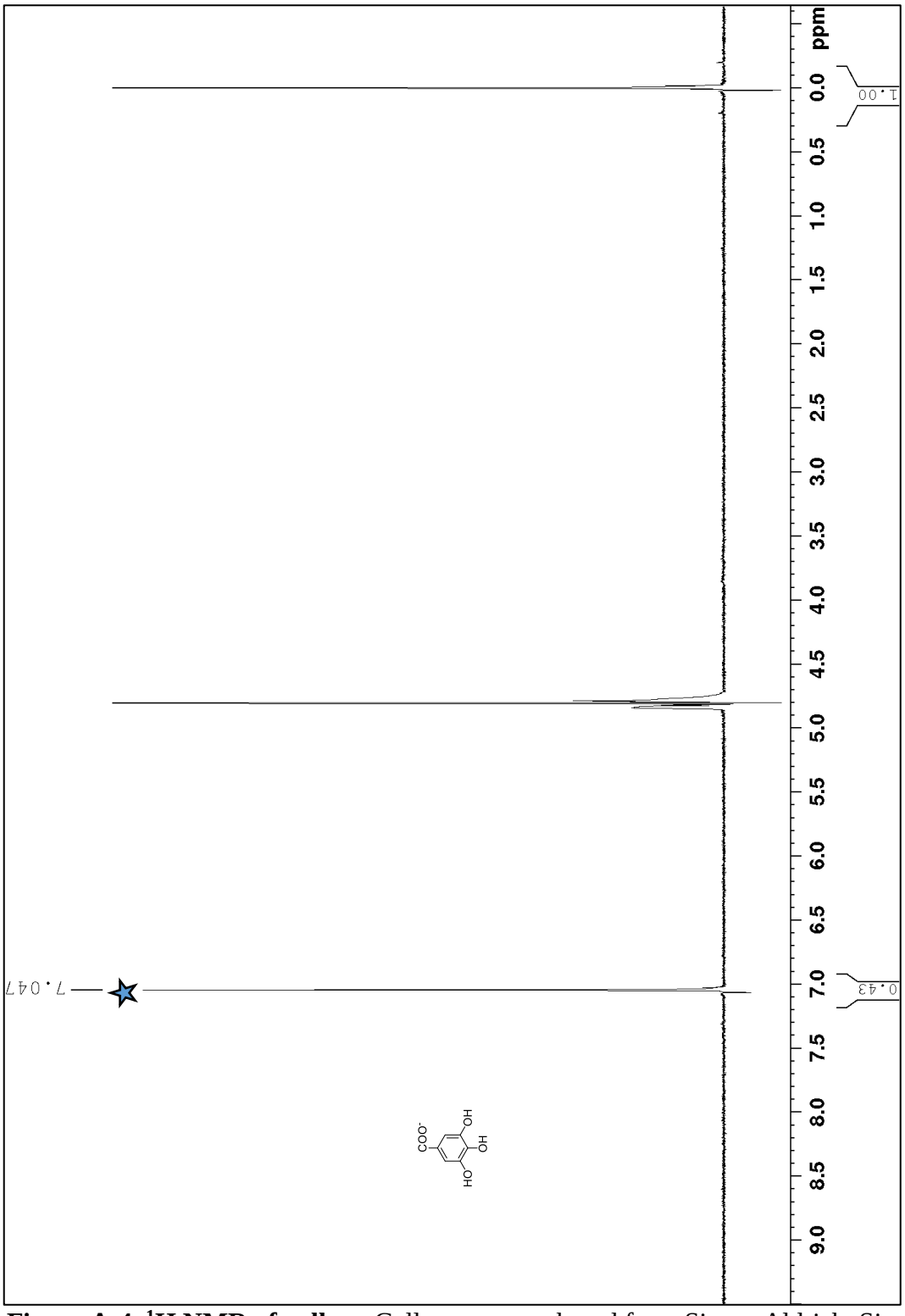

Figure A-4. ^{1}H NMR of gallate. Gallate was purchased from Sigma-Aldrich. Signal marked with star was used for quantification, response factor: 23.21 mM/intergration unit.

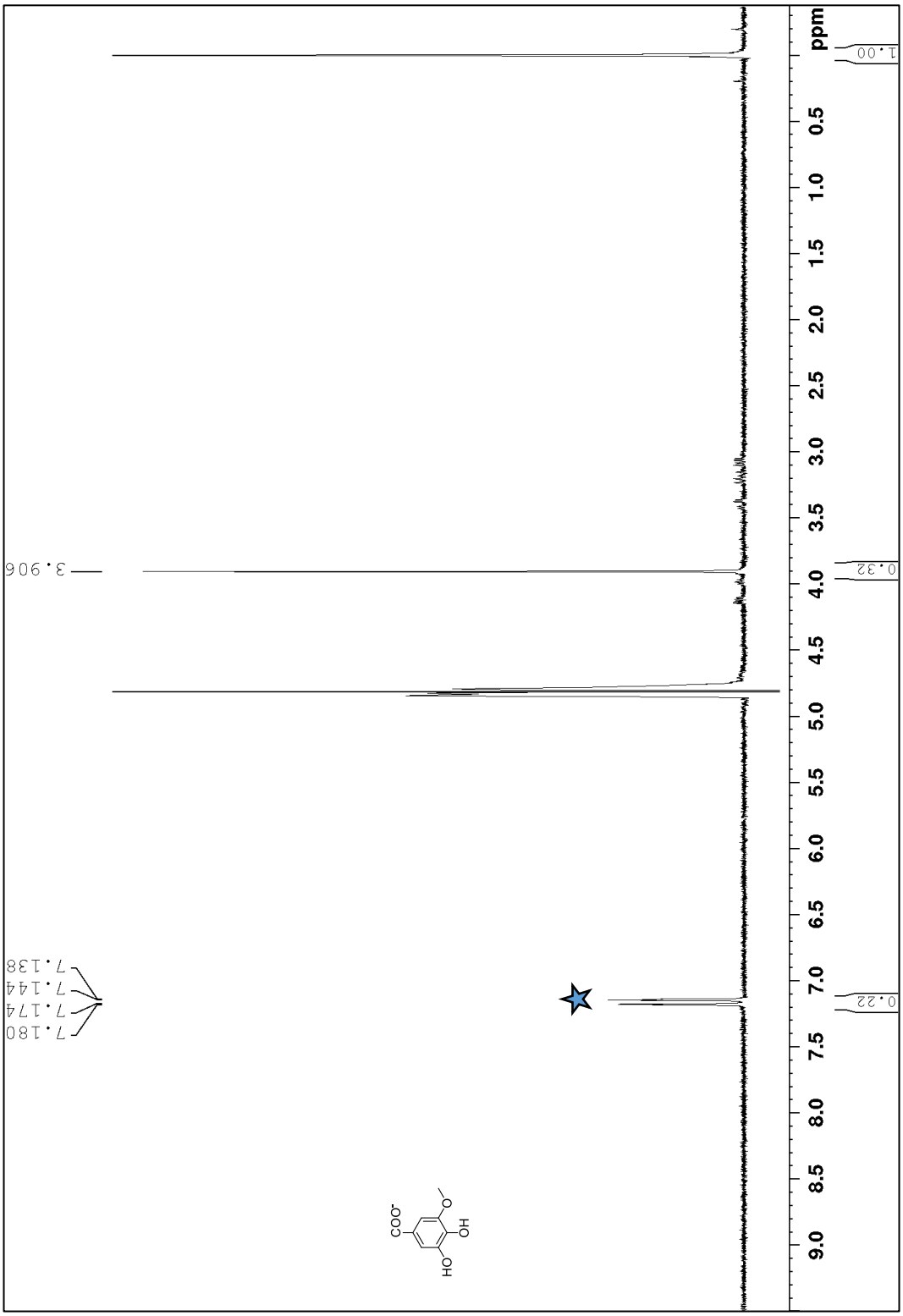

Figure A-5. ^{1}H NMR of 3OMG. 3OMG was purchased from Sigma-Aldrich. Signal marked with star was used for quantification, response factor: 22.97 mM/intergration unit.

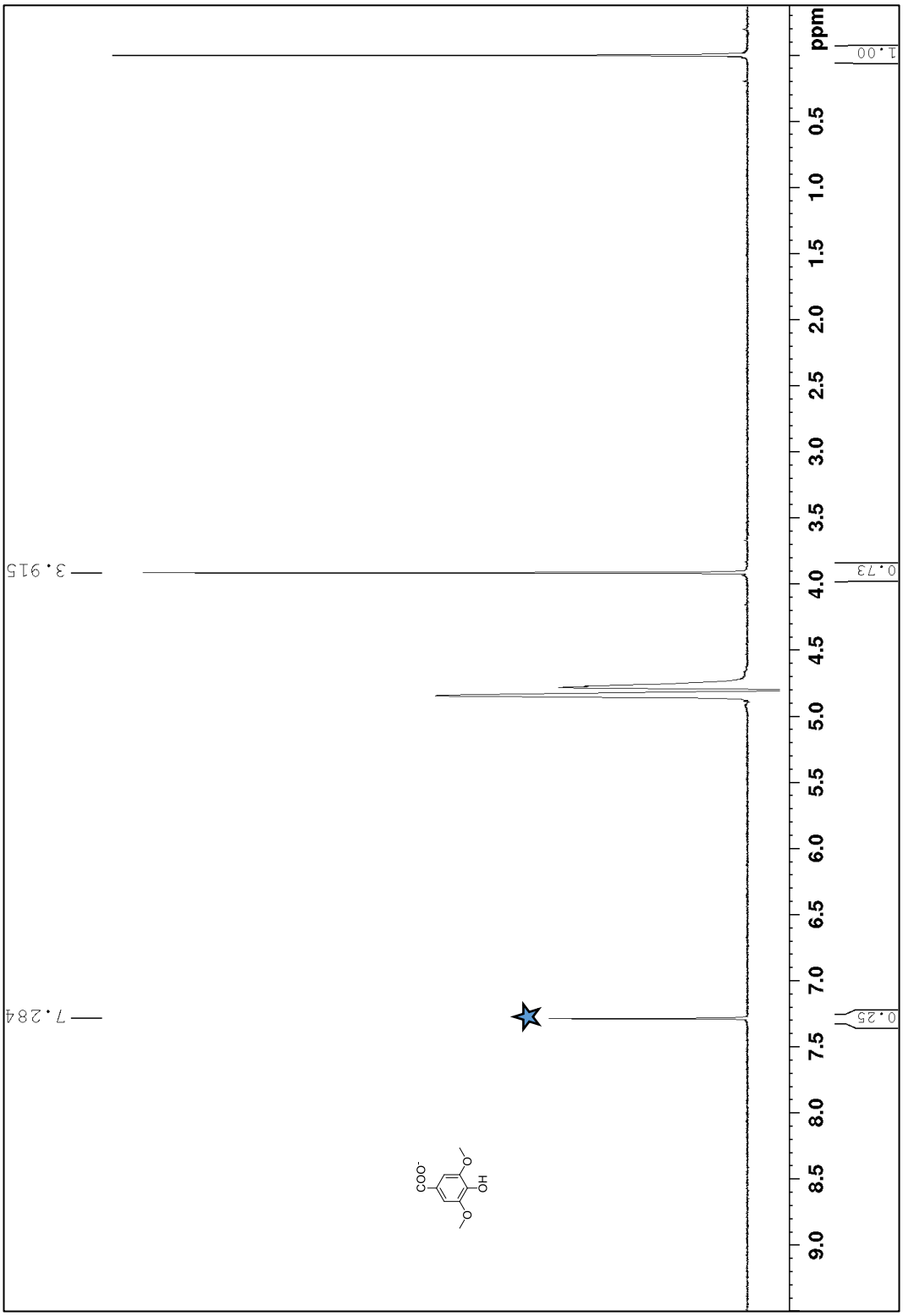

Figure A-6. ^{1}H NMR of syringate. Syringate was purchased from Sigma-Aldrich. Signal marked with star was used for quantification, response factor: 21.25 mM/intergration unit.

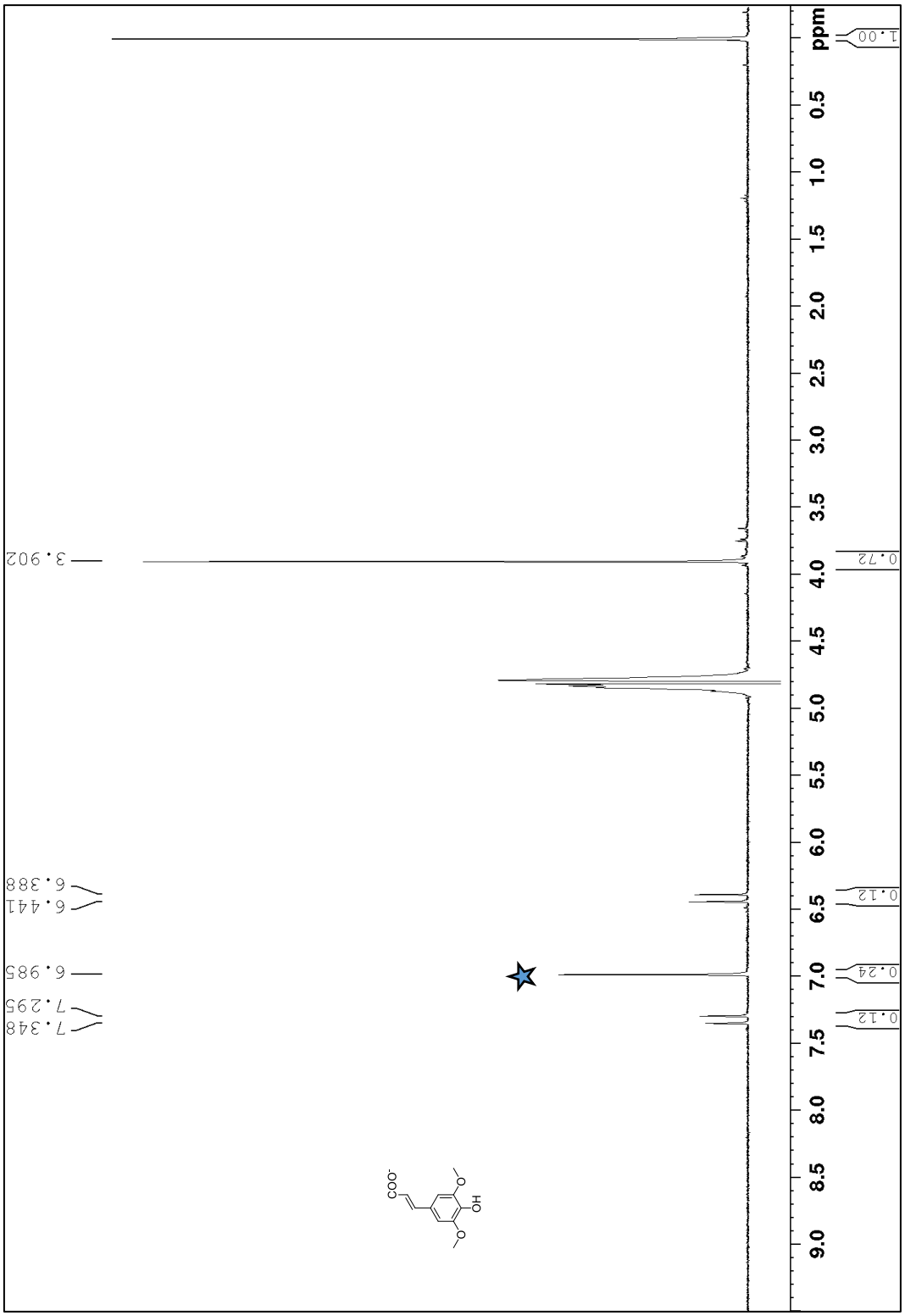

Figure A-7. ^{1}H NMR of sinapate. Sinapate was purchased from Sigma-Aldrich. Signal marked with star was used for quantification, response factor: 46.34 mM/intergration unit.

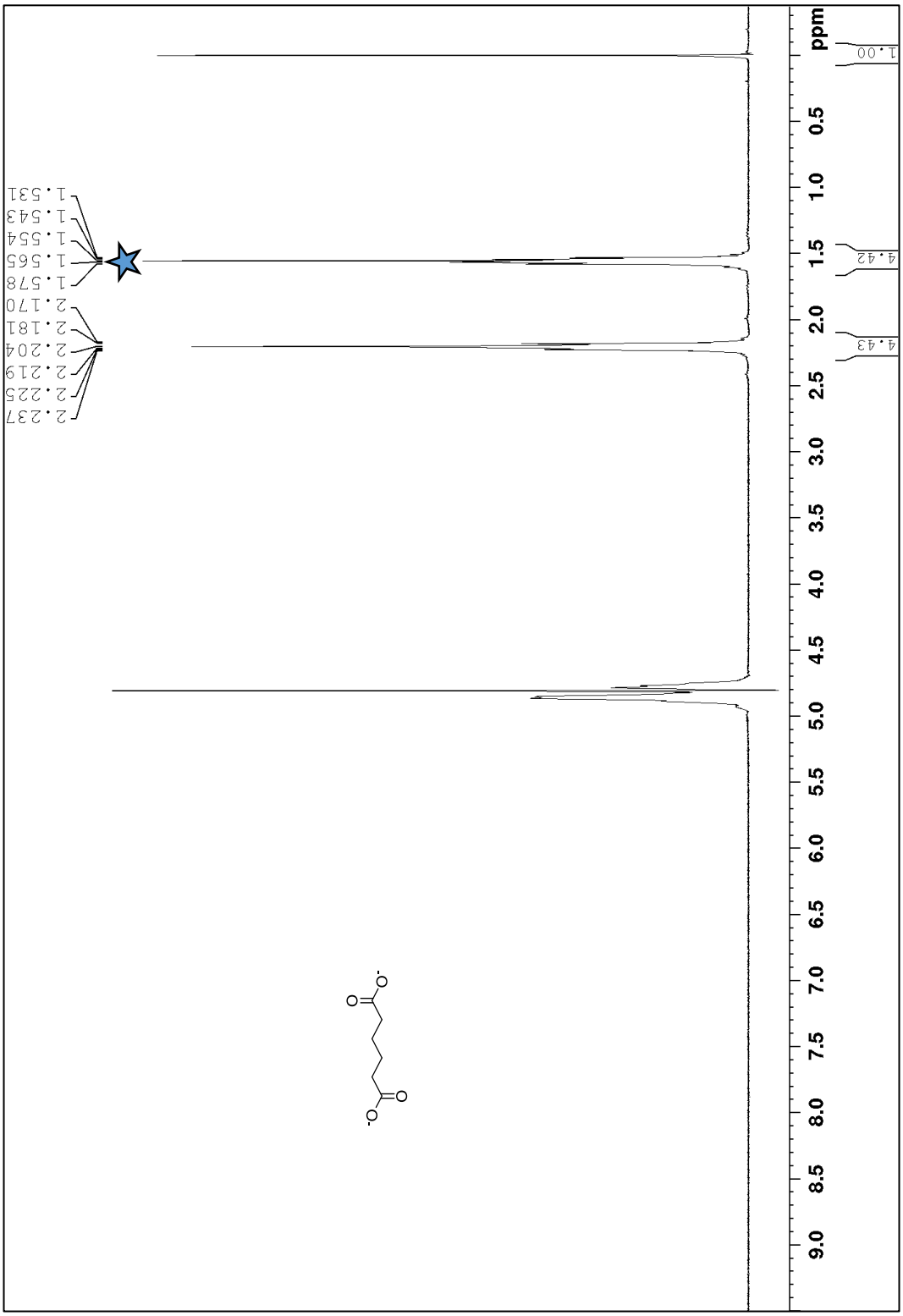

Figure A-7. ^{1}H NMR of adipate. Adipate was purchased from Sigma-Aldrich. Signal marked with star was used for quantification, response factor: 9.56 mM/intergration unit.

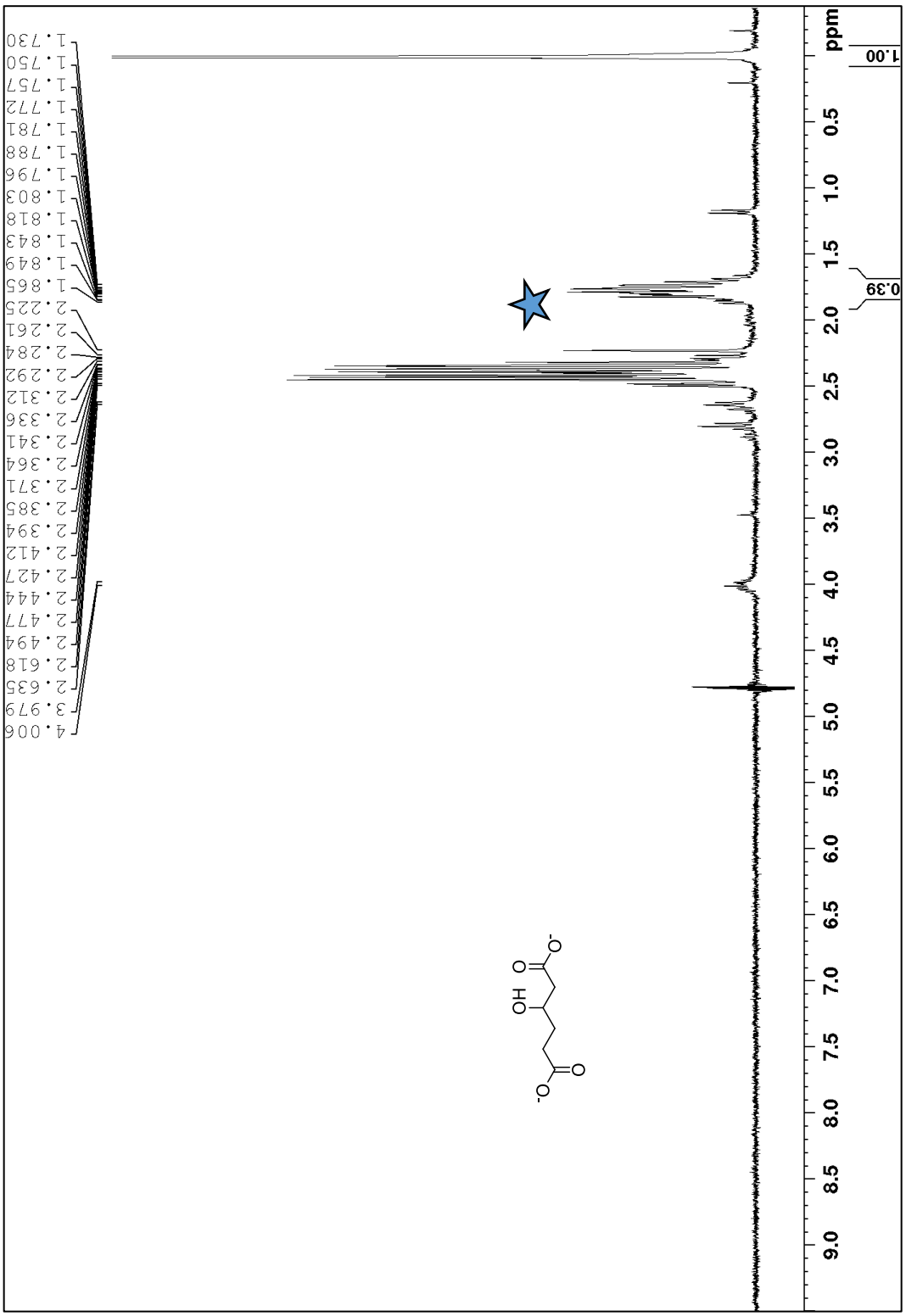

Figure A-8. ^{1}H NMR of 3-hydroxyadipate. 3-hydroxyadipate was synthesized from β-ketoadipate by chemical reduction. Signal marked with star used for quantification, response factor: 23.33 mM/intergration unit.

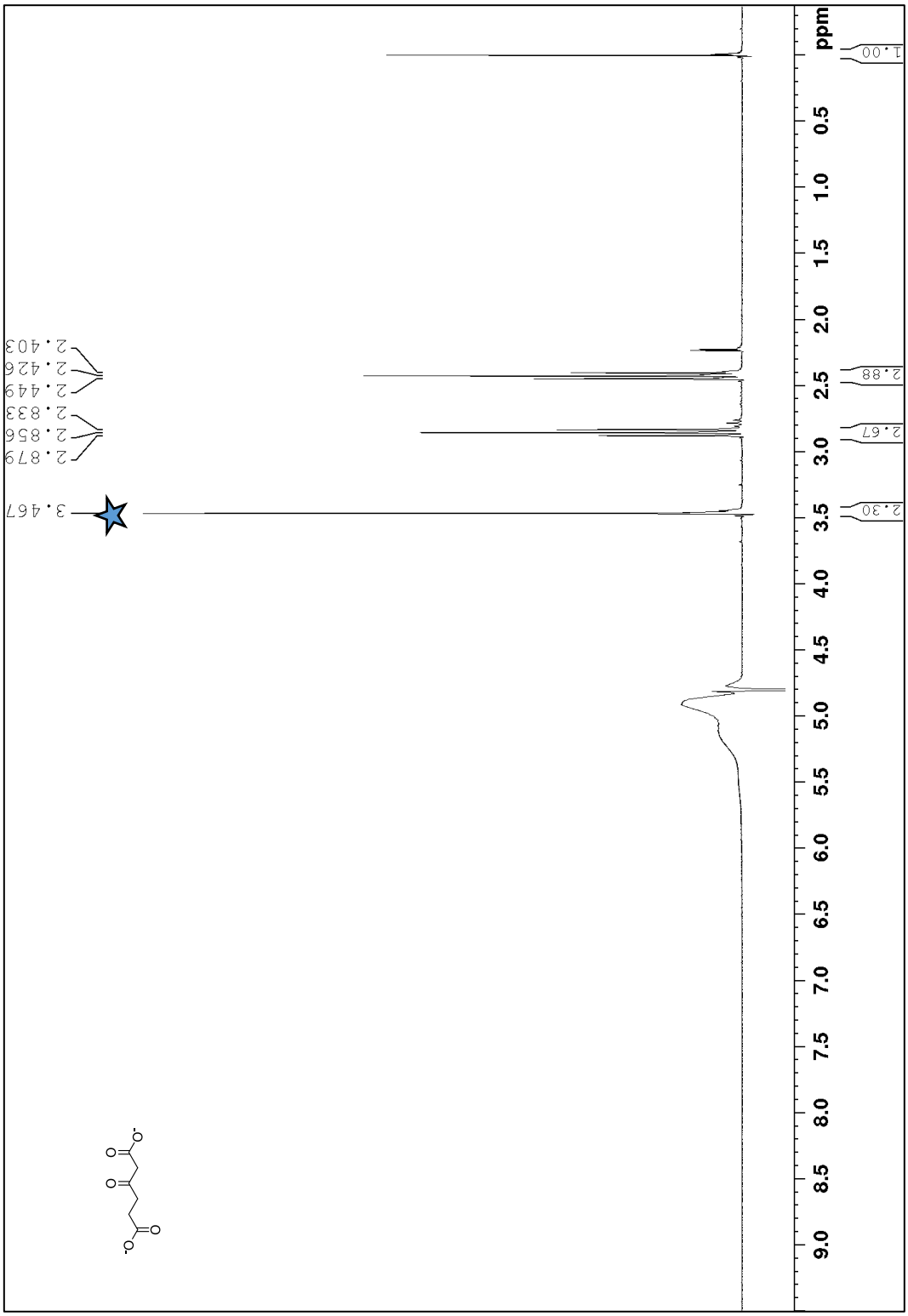

Figure A-9. ^{1}H NMR of β-ketoadipate. The β-ketoadipate was synthesized using a *P. putida* Δ3 catalyst . Signal marked with star used for quantification, response factor: 23.33 mM/intergration unit.

Appendix II – Plasmid and primers

Table A1: Plasmids constructed

Plasmid Name
pBBR-P_{tac}-sfGFP
pBBR-P_{A1}-sfGFP
pSEVA621-P_{tac}-sfGFP
pSEVA621-P_{A1}-sfGFP
pSEVA651-P_{tac}-sfGFP
pSEVA651-P_{A1}-sfGFP
pBBR-P_J-sfGFP
pBBR-P_N-sfGFP
pET28a-P_{lac}-VanAB
pBBR-P_{lac}-VanAB
pK19-mobsacB-ΔpcaF
pK19-mobsacB-ΔpaaJ
pK19-mobsacB-Δcrc
pK19-mobsacB-ΔpcaF ::Ptac-PaaFH-TdTer

Table A2: Primers used

Name	Sequence	Purpose
pET28vAB-F	cttccaatccgcacatatgtaccccaaaaa	Cloning of pET28a-VanAB
pet28vAB-R	ggtggtggtgctcgagtcagatgtccagca	Cloning of pET28a-VanAB
pET28vAB-Seq	gccgtttcaccccaccta	sequencing of pET28a-VanAB
pET28vAB-Seq2	ttgacgagcagccggaaa	sequencing of pET28a-VanAB
pBBR-DesA-F	gcaagaggagaagtcgacatgtcccagaccctagagcag	Amplification of DesA for SLIC into pBBR vector
pBBR-DesA-R	actagtaagcttcctaggttacttcttggtgcgccagccctc	Amplification of DesA for SLIC into pBBR vector
pBBR-LigM-F	gcaagaggagaagtcgacatggcggcaaagaacctcgaag	Amplification of LigM for SLIC into pBBR vector
pBBR-LigM-R	actagtaagcttcctaggttagcgagcggtgcgccagccttc	Amplification of LigM for SLIC into pBBR vector
pBBR-FerA-F	gcaagaggagaagtcgacatgaccggaacgagtctttc	Amplification of FerA for SLIC into pBBR vector
pBBR-FerA-R	actagtaagcttcctaggtcaatccacgagcatcaacgcgtc	Amplification of FerA for SLIC into pBBR vector
pBBR-LigV-FerB-F	gcaagaggagaagtcgacatgcagtttgaacgcatcaatc	Amplification of LigV-FerB for SLIC into pBBR vector
pBBR-LigV-FerB-R	actagtaagcttcctaggtcagcccttgaccttcgacgtgtc	Amplification of LigV-FerB for SLIC into pBBR vector

FerA seq primer	acagttccgcaagccaca	Sequencing of pBBR-FerA construct
ligV-ferB seq primer	tcggcaggatcatcgcaaa	sequencing of pBBR-ligV-ferB construct
PN25tetO-1	ttcgtcttcacctctagaaaatcataaaaaatttatttgcttc	Assembly of pN promoter for SLIC into vector
PN25tetO-2	actctattatactctatcactgatagggaagcaaataaattt	Assembly of pN promoter for SLIC into vector
PN25tetO-3	agagtataatagagtcgaattgttagcggagaagaatttcac	Assembly of pN promoter for SLIC into vector
PN25tetO-4	acttctcctcttcgctagcgaattctgtgtgaaattcttctccg	Assembly of pN promoter for SLIC into vector
PJ5-1	ttcgtcttcacctctagaagcggatataaaaaccgttat	Assembly of pJ promoter for SLIC into vector
PJ5-2	tattctaaatttccacctgtgtcaataacggtttttata	Assembly of pJ promoter for SLIC into vector
PJ5-3	tggaaatttagaaatatactgttagtaaacctaatggatc	Assembly of pJ promoter for SLIC into vector
PJ5-4	acttctcctcttgctagcaaggtcgatccattaggttta	Assembly of pJ promoter for SLIC into vector
5-pcaF-Up	catgattacgccaagcttgcatgctgggtattggccgcttgg	Amplification of Upstream homologous region of pcaF for pK19 vector construction
3-pcaF-UP	gtacaggtcacatcaggcttctcctgccagctggccatg	Amplification of Upstream homologous region of pcaF for pK19 vector construction
5-pcaF-DOWN	aagcctgatgtgacctgtaccggcctcttcgcggggaag	Amplification of downstream homologous region of pcaF for pK19 vector construction
3-pcaF-DOWN	acgacggccagtgaattcatcatcagggagccgaagcacatcatc	Amplification of downstream homologous region of pcaF for pK19 vector construction
5-pcaF-UP-V	ctgctagccacgctggtgctcgtc	Upstream primer for pcaF deletion check
5-pcaF-DOWN-V	cagcgctacttcactcatgtaggtg	downstream primer for pcaF deletion check
5-paaJ-Up	catgattacgccaagcttcgagagccgctaccgcccttccctg	Amplification of Upstream homologous region of paaJ for pK19 vector construction
3-paaJ-Up	gaaccgctcacatcttgcgtctcctgcgccagcac	Amplification of Upstream homologous region of paaJ for pK19 vector construction
5-paaJ-down	cgcaagatgtgagcggttcagaccctgcgcttgttaccgaactg	Amplification of downstream homologous region of paaJ for pK19 vector construction
3-paaJ-down	acgacggccagtgaattcgtaggacacatgcaccttgtcacctttg	Amplification of downstream homologous region of paaJ for pK19 vector construction
5-paaJ-Up-V	catgcgcgccggcgtcaattac	Upstream primer for paaJ deletion check
3-paaJ-down-V	gacggggtgaccatgatgatgtc	downstream primer for paaJ deletion check
5-CRC-Up	catgattacgccaagcttgatctgcatgacctcacgaatg	Amplification of Upstream homologous region of CRC for pK19 vector construction
3-CRC-UP	agccccaatggccttttacataaatggccccataaatctcgtg	Amplification of Upstream homologous region of CRC for pK19 vector construction
5-CRC-down	tttatggggccatttatgtaaaaggccattggggctgcattg	Amplification of downstream homologous region of CRC for pK19 vector construction
3-CRC-down	acgacggccagtgaattccgaaggcgcaccgttccagccggaag	Amplification of downstream homologous region of CRC for pK19 vector construction
5-CRC-Up-V	gtggatcgtcagccaggaactccag	Upstream primer for CRC deletion check
3-CRC-down-V	gtaggcatgtatcagggcgaagcggtg	downstream primer for CRC deletion check

GA5-UP-pcaF-PT	cagctatgacatgattacgccaagcttatgctgggtattggccgc	Amplification of upstream homologous fragment to construct pk19 vector for PT insertion
GA5-down-pcaF-PT	gtgcgccttgagcgacacgaactcgagcaggcttctcctgccagc	Amplification of upstream homologous fragment to construct pk19 vector for PT insertion
Ga3-up-pcaF-P	gcgccaaagcctaggaagcttactagttgacctgtaccggcctct	Amplification of upstream homologous fragment to construct pk19 vector for PT insertion
Ga3-downpcaF-PT	cgttgtaaaacgacggccagtgaattctcatcagggagccgaagc	Amplification of upstream homologous fragment to construct pk19 vector for PT insertion

References

1. Robinson, P. R.; Hsu, C. S. Petroleum and Its Products. In *Handbook of Industrial Chemistry and Biotechnology*; Kent, J. A., Bommaraju, T. V. and Barnicki, S. D., Eds.; 2017; pp 13-106.

2. Ragauskas, A. J.; Beckham, G. T.; Biddy, M. J.; Chandra, R.; Chen, F.; Davis, M. F.; Davison, B. H.; Dixon, R. A.; Gilna, P.; Keller, M.; Langan, P.; Naskar, A. K.; Saddler, J. N.; Tschaplinski, T. J.; Tuskan, G. A.; Wyman, C. E. Lignin valorization: improving lignin processing in the biorefinery. *Science.* **2014**, *344*, 709.

3. Boerjan, W.; Ralph, J.; Baucher, M. Lignin biosynthesis. *Annual Review of Plant Biology.* **2003**, *54*, 519.

4. Pandey, M. P.; Kim, C. S. Lignin Depolymerization and Conversion: A Review of Thermochemical Methods. *Chemical Engineering & Technology.* **2011**, *34*, 29-41.

5. Nelson, K. E.; Weinel, C.; Paulsen, I. T.; Dodson, R. J.; Hilbert, H.; Martins dos Santos, V A P; Fouts, D. E.; Gill, S. R.; Pop, M.; Holmes, M.; Brinkac, L.; Beanan, M.; DeBoy, R. T.; Daugherty, S.; Kolonay, J.; Madupu, R.; Nelson, W.; White, O.; Peterson, J.; Khouri, H.; Hance, I.; Chris Lee, P.; Holtzapple, E.; Scanlan, D.; Tran, K.; Moazzez, A.; Utterback, T.; Rizzo, M.; Lee, K.; Kosack, D.; Moestl, D.; Wedler, H.; Lauber, J.; Stjepandic, D.; Hoheisel, J.; Straetz, M.; Heim, S.; Kiewitz, C.; Eisen, J. A.; Timmis, K. N.; Düsterhöft, A.; Tümmler, B.; Fraser, C. M. Complete genome sequence and comparative analysis of the metabolically versatile Pseudomonas putida KT2440. *Environmental Microbiology.* **2002**, *4*, 799-808.

6. Dos Santos, V A P Martins; Heim, S.; Moore, E. R. B.; Strätz, M.; Timmis, K. N. Insights into the genomic basis of niche specificity of Pseudomonas putida KT2440. *Environmental Microbiology.* **2004**, *6*, 1264-1286.

7. Harwood, C. S.; Parales, R. E. The β-ketoadipate pathway and the biology of self-identity. *Annual Review of Microbiology.* **1996**, *50*, 553-590.

8. Plaggenborg, R.; Overhage, J.; Steinbuchel, A.; Priefert, H. Functional analyses of genes involved in the metabolism
of ferulic acid in Pseudomonas putida KT2440. *Applied Microbiology and Biotechnology.* **2003**, *61*, 528-535.

9. Nogales, J.; Canales, Á; Jiménez-Barbero, J.; Serra, B.; Pingarrón, J. M.; García, J. L.; Díaz, E. Unravelling the gallic acid degradation pathway in bacteria: the gal cluster from Pseudomonas putida. *Molecular Microbiology.* **2011**, *79*, 359-374.

10. Hughes, G.; Lewis, J. Introduction: Biocatalysis in Industry. *Chemical Reviews.* **2018**, *118*, 1-3.

11. Dhillon, S. Sitagliptin: A Review of its Use in the Management of Type 2 Diabetes Mellitus. *Drugs.* **2010**, *70*, 489-512.

12. Patrick E. McGovern; Juzhong Zhang; Jigen Tang; Zhiqing Zhang; Gretchen R. Hall; Robert A. Moreau; Alberto Nuñez; Eric D. Butrym; Michael P. Richards; Chen-shan Wang; Guangsheng Cheng; Zhijun Zhao; Changsui Wang; Ofer Bar-Yosef Fermented Beverages of Pre- and Proto-Historic China. *Proceedings of the National Academy of Sciences of the United States of America.* **2004**, *101*, 17593-17598.

13. Song, H.; Lee, S. Y. Production of succinic acid by bacterial fermentation. *Enzyme and Microbial Technology.* **2006**, *39*, 352-361.

14. Harry Yim; Robert Haselbeck; Wei Niu; Catherine Pujol-baxley; Anthony Burgard; Jeff Boldt; Julia Khandurina; John D Trawick; Robin E Osterhout; Rosary Stephen; Jazell Estadilla; Sy Teisan; H Brett Schreyer; Stefan Andrae; Tae Hoon Yang; Sang Yup Lee; Mark J Burk; Stephen Van Dien Metabolic engineering of Escherichia coli for direct production of 1,4-butanediol. *Nature Chemical Biology.* **2011**, *7*, 445-452.

15. Li, M.; Kildegaard, K. R.; Chen, Y.; Rodriguez, A.; Borodina, I.; Nielsen, J. De novo production of resveratrol from glucose or ethanol by engineered Saccharomyces cerevisiae. *Metabolic Engineering.* **2015**, *32*, 1-11.

16. Bart, J. C.; Cavallaro, S. Transiting from Adipic Acid to Bioadipic Acid. 1, Petroleum-Based Processes. *Industrial & Engineering Chemistry Research.* **2014**, *54*, 1-46.

17. Baker, I. Nylon. In *Fifty Materials That Make the World.* Springer, Cham: 2018; pp 143-146.

18. AJ, M. Carcinogenicity of benzene, toluene and xylene: epidemiological and experimental evidence. *IARC Scientific Publications.* **1988**, *85*, 3-18.

19. Shimizu, A.; Tanaka, K.; Fujimori, M. Abatement technologies for N2O emissions in the adipic acid industry. *Chemosphere Global Change Science.* **2000**, *2*, 425-436.

20. Wei Niu; K M Draths; J W Frost Benzene-Free Synthesis of Adipic Acid. *Biotechnology Progress.* **2002**, *18*, 201-211.

21. Curran, K. A.; Leavitt, J. M.; Karim, A. S.; Alper, H. S. Metabolic engineering of muconic acid production in Saccharomyces cerevisiae. *Metabolic Engineering.* **2013**, *15*, 55-66.

22. Bart, J. C. J.; Cavallaro, S. Transiting from Adipic Acid to Bioadipic Acid. Part II. Biosynthetic Pathways. *Industrial & Engineering Chemistry Research.* **2015**, *54*, 567-576.

23. Zhao, M.; Huang, D.; Zhang, X.; Koffas, M. A. G.; Zhou, J.; Deng, Y. Metabolic engineering of Escherichia coli for producing adipic acid through the reverse adipate-degradation pathway. *Metabolic Engineering.* **2018**, *47*, 254-262.

24. Raj, K.; Partow, S.; Correia, K.; Khusnutdinova, A. N.; Yakunin, A. F.; Mahadevan, R. Biocatalytic production of adipic acid from glucose using engineered Saccharomyces cerevisiae. *Metabolic Engineering Communications.* **2018**, *6*, 28-32.

25. Maxwell, P. C. United States Patent US4731328A, 1983.

26. Nogales, J.; Canales, Á; Jiménez-Barbero, J.; Serra, B.; Pingarrón, J. M.; García, J. L.; Díaz, E. Unravelling the gallic acid degradation pathway in bacteria: the gal cluster from Pseudomonas putida. *Molecular Microbiology.* **2011**, *79*, 359-374.

27. Barry, K. P.; Cohn, E. F.; Ngu, A.; Taylor, E. A. Improving alternate lignin catabolite utilization of LigAB from Sphingobium sp. strain SYK-6 through site directed mutagenesis. *Process Biochemistry.* **2015**, *50*, 1634-1639.

28. Cecil, J. H.; Garcia, D. C.; Giannone, R. J.; Michener, J. K. Rapid, parallel identification of pathways for catabolism of lignin-derived aromatic compounds in Novosphingobium aromaticivorans. *Applied and Environmental Microbiology.* **2018**, *84*.

29. Morawski, B.; Segura, A.; Ornston, L. N. Repression of Acinetobacter vanillate demethylase synthesis by VanR, a member of the GntR family of transcriptional regulators. *FEMS Microbiology Letters.* **2000**, *187*, 65-68.

30. Kambiz Morabbi Heravi; Julian Lange; Hildegard Watzlawick; Jörn Kalinowski; Josef Altenbuchner Transcriptional Regulation of the Vanillate Utilization Genes (vanABKOperon) of Corynebacterium glutamicum by VanR, a PadR-Like Repressor. *Journal of Bacteriology.* **2015**, *197*, 959-972.

31. Cheong, S.; Clomburg, J. M.; Gonzalez, R. Energy- and carbon-efficient synthesis of functionalized small molecules in bacteria using non-decarboxylative Claisen condensation reactions. *Nature Biotechnology.* **2016**, *34*, 556-561.

32. Gracia Morales; Juan Francisco Linares; Ana Beloso; Juan Pablo Albar; José Luis Martínez; Fernando Rojo The Pseudomonas putida Crc Global Regulator Controls the Expression of Genes from Several Chromosomal Catabolic Pathways for Aromatic Compounds. *Journal of Bacteriology.* **2004**, *186*, 1337-1344.

33. Li, M. Z.; Elledge, S. J. Harnessing homologous recombination in vitro to generate recombinant DNA via SLIC. *Nature Methods.* **2007**, *4*, 251-256.